ERDC/CRREL TR-06-11

Cold Regions Research
and Engineering Laboratory

US Army Corps
of Engineers®
Engineer Research and
Development Center

# Double Lap Shear Testing of Coating Modified Ice Adhesion to Liquid Oxygen Feed Line Bracket, Space Shuttle External Tank

M.G. Ferrick, N.D. Mulherin, R.B. Haehnel, B.A. Coutermarsh,
G.D. Durell, T.J. Tantillo, T.L. St. Clair, E.S. Weiser, R.J. Cano,
T.M. Smith, and E.C. Martinez

May 2006

**Cover:** STS 114 tanking test showing upper $LO_2$ feed line bracket viewed from below, with the underside of the orbiter visible on the left (Photo by Trent. Smith).

ERDC/CRREL TR-06-11
May 2006

# Double Lap Shear Testing of Coating Modified Ice Adhesion to Liquid Oxygen Feed Line Bracket, Space Shuttle External Tank

M.G. Ferrick, N.D. Mulherin, R.B. Haehnel, B.A. Coutermarsh, G.D. Durell, and T.J. Tantillo

*Cold Regions Research and Engineering Laboratory*
*U.S. Army Engineer Research and Development Center*
*72 Lyme Rd*
*Hanover, NH 03755*

T.L. St. Clair

*National Institute of Aerospace*
*Hampton, VA*

E.S. Weiser and R.J. Cano

*NASA Langley Research Center*
*Hampton, VA*

T.M. Smith

*NASA John F. Kennedy Space Center*
*KSC, FL*

E.C. Martinez

*Lockheed Martin Space Systems*
*MSFC, AL*

Final report



Prepared for National Aeronautics and Space Administration

Under NASA order NNL05AA401

**Abstract:** The brackets that secure the liquid oxygen feed line to the external tank are known locations of frost and ice growth during the period following fuel loading. This experiment quantified the reduced adhesion when ice phobic coatings were applied to test coupons simulating the bracket surface. Double lap shear testing of coated and uncoated coupons provided robust test specimens and consistent load response patterns with exceptional resolution. For these tests ice was grown as strong and consistently as possible, subjected to temperature decreases comparable to those of the prototype bracket, and tested at a controlled temperature of –112°C. The tests evolved in three phases, with uncoated controls included in each group of tested samples. The first phase of testing evaluated a wide range of coatings, and showed that Rain-X mixed with MP-55 powdered Teflon (RXM) was an outstanding coating to reduce ice adhesion to Koropon coated aluminum. However, significant amounts of coating were retained on the ice surface following each test, indicating failure in the coating and potential loss of effectiveness with repeated ice formation and release. Phase 2 evaluated potential modifications to RXM that might maintain effectiveness and enhance durability. However, the modified RXM mixtures did not improve the ice adhesion performance or coating durability. Phase 3 evaluated the effects of handling, application, resistance to weathering by water, and durability of the RXM coating. Coating material was again progressively lost through the repeat test cycles, but performance generally improved. Results also indicated that cure times longer than 1.5 hr prior to coating disturbance are needed for optimal performance. The MP55 remaining on the surface of three coupons after three cycles of testing, and on one untested coupon from the same group, was measured with XPS. The tested coupons retained slightly less MP55 than the untested coupon, indicating a minor loss of coating. Contact angle analysis of these same coupons showed that the hydrophobic performance of the tested surfaces was largely preserved. Scanning electron microscopy with an energy dispersive spectroscopy elemental map indicated that the MP-55 was evenly dispersed throughout the coated surface, and abrasive wiping did not remove a significant portion of the Teflon. Follow-up studies to refine the optimal coating formulation, mixing, and application procedures, including cure time, are necessary. Phase 1 testing indicated superiority of UF-8TA powdered Teflon over MP-55 when mixed with Braycote. As UF-8TA was not mixed with Rain-X, this change in Teflon powder might offer performance and consistency improvements to the coating. Also, reaction processes and environmental durability of the final coating must be better understood. Double lap shear testing and XPS analysis can quantify ice adhesion and coating profile thickness changes with cycling, and is a proven approach to resolve these remaining issues.

# Contents

# Figures and Tables

## Figures

## Tables

# Preface

This report was prepared by Michael Ferrick, Nathan Mulherin, Robert Haehnel, Barry Coutermarsh, Glenn Durell, and Thomas Tantillo, U.S. Army Engineer Research and Development Center, Cold Regions Research and Engineering Laboratory; Terry St. Clair, National Institute of Aerospace; Erik Weiser, and Roberto Cano, NASA Langley Research Center; Trent Smith, NASA John F. Kennedy Space Center; and Eloy Martinez, Lockheed Martin Space Systems.

The authors thank Leslie Curtis and Michael Kirsch of NASA-NESC for reviews of this report, and for skillful leadership and coordination of all the work on coating development to reduce ice adhesion. They also thank Anne St. Clair for help with coating samples. Many members of the NASA ice mitigation team contributed on numerous telecons to the success of this work, and they thank them all for these contributions. Funding to support the CRREL staff on this project was provided under NASA order number NNL05AA401, and is gratefully acknowledged.

This report was prepared under the general supervision of Terry Sobecki, Chief, Environmental Sciences Branch; Lance Hansen, Acting Deputy Director; and James Wuebben, Acting Director, CRREL. The Commander and Executive Director of the Engineer Research and Development Center is COL James R. Rowen. The Director is Dr. James R. Houston.

# Unit Conversion Factors

| Multiply | By | To Obtain |
|---|---|---|
| angstroms | 0.1 | nanometers |
| degrees Fahrenheit | (F–32)/1.8 | degrees Celsius |
| inches | 0.0254 | meters |
| inch-pounds (force) | 0.1129848 | newton meters |
| microns | $1.0 \times 10^{-6}$ | meters |
| pounds (force) | 4.448222 | newtons |
| pounds (mass) | 0.45359237 | kilograms |

# Executive Summary

The brackets that secure the liquid oxygen ($LO_2$) feed line to the external tank are known locations of frost and ice growth during the pre-launch period following fuel loading. These aluminum brackets are in contact with the cryogenic liquid fuel tanks, and the exposed surface is uninsulated to allow space for thermal flexing of the feed line. Ice grows on the brackets, and if liberated, this "bracket ice" is a debris source that is a threat to the shuttle elements. However, ice release at low speed, very early in the launch, would minimize the potential damage. The primary goal of this experimental program was to quantify the reduction in adhesion caused by ice phobic coatings that could be applied to the bracket surface. These coatings may also improve the ice release at other locations on the shuttle. Other goals of the program were to evaluate coating consistency and durability.

## Overview of Experiment and Test Conditions

Preliminary double lap shear tests (ASTM [2002] D3528-96) of uncoated coupons simulating the bracket surface provided robust test specimens, and consistent load response patterns with exceptional resolution. On the basis of these results, double lap shear testing of coated coupons was initiated at the U.S. Army Engineer Research and Development Center's Cold Regions Research and Engineering Laboratory (CRREL). Measured $LO_2$ bracket temperatures indicated that most of the temperature decrease occurred over 6 hours, followed by an asymptotic approach to a minimum of –112°C (–170°F). For these tests ice was grown as strong and consistently as possible, and then subjected to temperature decreases comparable to those of the prototype, ending at a stable test temperature of –112°C.

The double lap shear-testing program evolved in three phases. Each group of samples tested in all phases of the program included uncoated controls. The first phase of testing evaluated the performance of a wide range of candidate coatings. Phase 2 investigations evaluated potential modifications to the best phase 1 coating, Rain-X mixed with maximum MP-55 powdered Teflon (RXM), which might maintain effectiveness and enhance durability. Phase 3 evaluated the effects of handling, application, resistance to weathering by water, and durability of the RXM coating.

## Test Results

Phase 1 tests showed that RXM was an outstanding coating to reduce the adhesion of ice to Koropon coated aluminum at cryogenic temperatures. However, significant amounts of coating were retained on the ice surface following each test cycle, indicating failure in the coating and potential loss of effectiveness with repeated ice formation and release. Even with this durability question, outstanding performance and indications of durability were promising. The addition of DF 1040 in phase 2 to the original RXM mixture did not improve the ice adhesion performance or coating durability. Coating material was again lost in each test cycle with all DF 1040 mixes. Results also indicated that the DC 1200 primer used in phase 2 slightly degraded the overall performance of the coating. A progressive loss of coating material also occurred through the test cycles of phase 3. Phase-3 performance of the non-wiped coupons generally improved from cycle 1 to cycle 3. The corresponding wiped samples also improved with cycling, though the incremental decreases in work were smaller. Re-wetting the coating mixture with isopropyl alcohol (IPA) after drying and prior to use caused a small loss of performance, and subjecting the coating to a water stream after curing caused a slightly larger loss. Dried and re-wetted samples were wiped after only a 0.5-hour cure time, and developed much higher loads than all the other samples. The 1.5-hour cure prior to wiping of the other samples was much better, but still not adequate for optimal performance. The loss in performance caused by wiping the coating off was very sensitive to cure time, and longer times than those allowed here are needed prior to any coating disturbance.

## XPS, Contact Angle, and SEM-EDS Results

The MP55 remaining on the surface of three non-wiped coupons following three test cycles was measured with XPS and compared to similar measurements of a coupon from the same group that had never been tested. Surface chemistry of control coupons, both uncoated and coated with plain Rain-X, was also mapped with XPS. The surface compositions of the tested coupons were similar, but totally different from the controls. The tested coupons retained less MP55 than the untested coupon, indicating a minor loss of coating. These results are consistent with the observed coating loss with each test cycle, and suggest that the failure plane between the coupon and the ice occurs within the coating. Contact angle analysis along these same coupons concurred with the XPS results, showing that the hydro-

phobic performance of the surfaces was largely preserved after three test cycles.

Scanning electron microscopy (SEM), coupled with an energy dispersive spectroscopy elemental map of fluorine, was used to visualize conditions on thinly RXM coated coupon surfaces. A test coupon was coated and cured for 2+ days prior to analysis, abrasive wiping, and re-analysis. The MP-55 was evenly dispersed throughout the coating on the surface of the non-wiped coupon, and abrasive wiping did not remove a significant portion of the Teflon from the surface. Measured MP-55 bead diameters fell below the wavelength of visible light, inferring that though the coating may appear to have been removed, it is still present. These SEM results verify the presence of MP-55 on the coupon surface following abrasion, and support those of the XPS and contact angle analyses.

## Recommendations

The results of this investigation suggest follow-up studies to refine the optimal coating formulation, mixing, and application procedures, including cure time. Overall consistency and performance in phase 1 indicated superiority of UF-8TA powdered Teflon over MP-55 when mixed with Braycote. As UF-8TA was not mixed with Rain-X, this change in Teflon powder might offer performance and consistency improvements to the coating. Also, reaction processes during curing and environmental durability must be better understood. Additional test cycles beyond those done in this program should eventually compromise the integrity and performance of the coating, and this limit is not yet known. Parallel double lap shear testing and XPS analysis can quantify ice adhesion and coating profile thickness changes with cycling, and is a proven approach to resolve these remaining issues.

# 1 Introduction

Ice is one form of debris from the external fuel tank of the space shuttle that can be liberated during launch, potentially causing damage to the shuttle elements. The brackets that secure the liquid oxygen ($LO_2$) feed line to the external tank are known locations of frost and ice growth during the pre-launch period that follows fuel loading. These aluminum brackets are in contact with the cryogenic liquid fuel tanks, and the exposed surfaces are uninsulated to allow space for thermal flexing of the feed line. Ice grows on the brackets primarily as a result of initial frost formation, followed by condensate rundown and subsequent freezing within the frost. If liberated, this bracket ice is a source of debris that is a threat to the shuttle elements. The locations of the feed line brackets are indicated in Figure 1. Figure 2 provides a close-up view of a bracket with ice present, and Figure 3 is an engineering drawing of the bracket with the exposed surface indicated in blue.

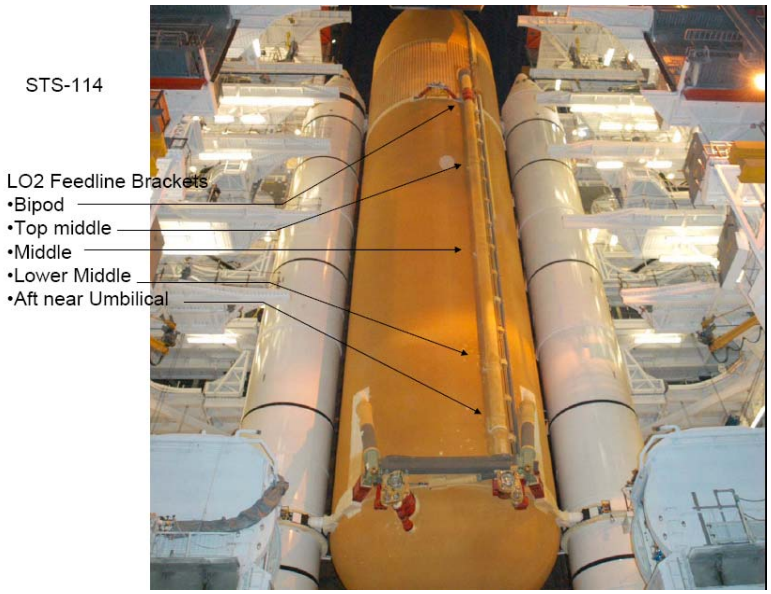


Figure 1. Locations of the liquid oxygen (LO2) feed line brackets on the external tank of the space shuttle.

The goal of this experimental program was to quantify the effect of many candidate coatings, each with distinct properties, on the force of bracket ice adhesion, and evaluate the consistency of coating performance and its durability. These candidate coatings could be applied to the bracket sur-

face and adjacent foam to reduce ice adhesion. The resulting ice release at low speed very early in the launch would minimize the damage potential to the shuttle elements. Other possible areas on the shuttle were identified later in the study that may also benefit from coating application and early ice release.

Figure 2. Ice frost on a $LO_2$ feed line bracket of the external tank.

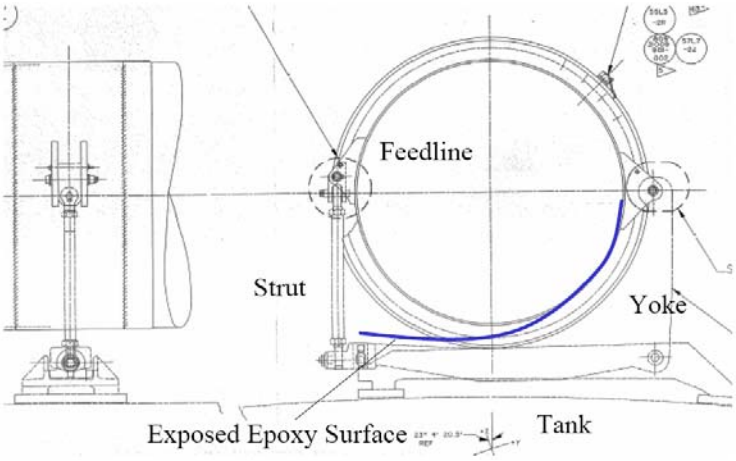


Figure 3. Engineering drawing of the feed line bracket and associated structures. The uninsulated surface is depicted in blue.

# 2 Development of the Experiment

Preliminary discussions of the NASA-NESC ice mitigation team led to selection of the single lap shear test, following ASTM (2003) D3164-03, as a simple experiment to evaluate and quantify candidate coating materials for their bracket ice release potential. Coupon size and shape for this test were designed at CRREL (Fig. 4), and coupons were produced by NASA-MSFC using aluminum painted with epoxy (Koropon) to simulate the exposed metal surface of the feed line bracket. The Koropon Primer is an amine-cured epoxy and the resulting coating possesses hydroxyl chemical groups (moieties). Each test specimen was composed of two coupons bonded together by ice 0.125 in. thick with an area of 1 by 1 in.

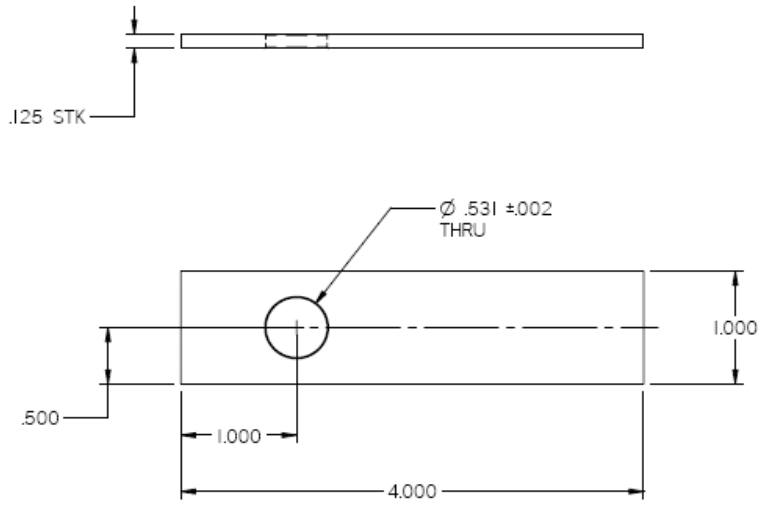


Figure 4. Engineering drawing of CRREL coupon design for ice adhesion testing.

Shear testing was performed on an MTS machine, which is a closed-loop electro-hydraulic servo-controlled system, in a temperature controlled test chamber (Fig. 5). A displacement transducer incorporated in the loading actuator was used to control the system and measure the deformation. The controller can be programmed for a constant deformation rate or series of constant rates. Because of the large load differences anticipated between the uncoated controls and the high performance coatings, two load cells in line with the loading actuator were used. This configuration provides greater measurement resolution and accuracy.


a. Wide view.

b. Close view.

Figure 5. Chamber cooled by liquid nitrogen for mechanical testing at controlled cryogenic temperatures. Both a and b show the cryo-gloves built into the front of the chamber for handling samples at extreme temperature.

The single lap coupon pairs were mounted in the MTS machine between the loading platens using a clevis and pin setup, and pulled longitudinally (Fig. 6). A data acquisition system collected and stored temperature, deformation, and load data through time. The data from each test were immediately analyzed for peak load and total work, and load–displacement, load–time and displacement–time data were plotted.

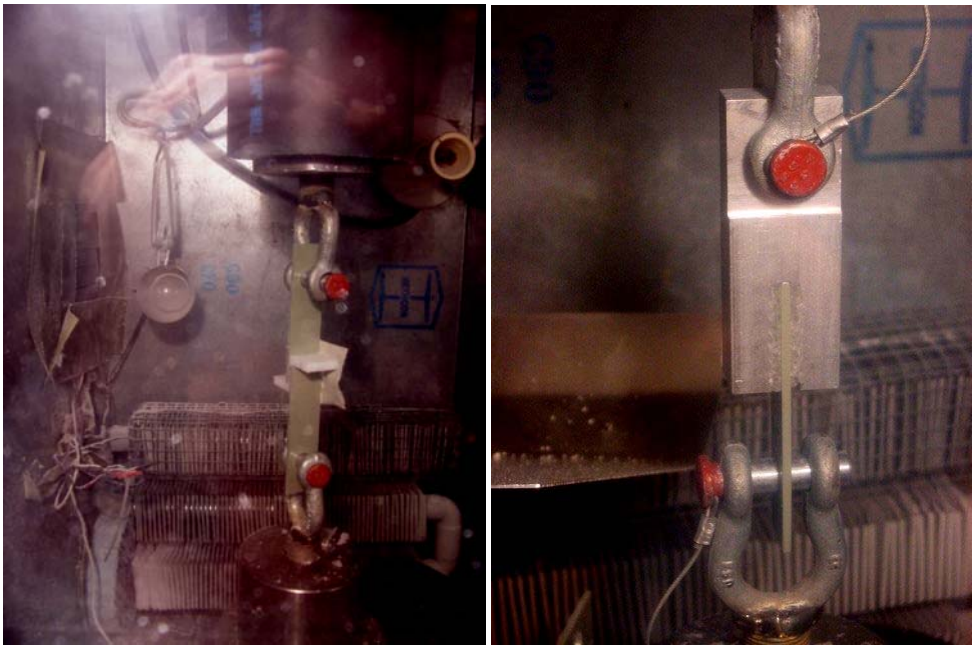

Figure 6. (left) Single lap shear specimen mounted in the MTS machine inside the test chamber, and (right) double lap shear specimen in the same configuration.

Preliminary singe lap shear testing of several sample groups was done with various modifications during late April and early May 2005. Failed samples were taken to a coldroom for inspection, correlation with test data, logging of characteristics, and photographs. The first problem encountered was that the ice bond between the coupon pairs was fragile, and many samples broke during handling prior to testing. Another problem was that the uncoated samples yielded maximum failure loads of less than 20 lbf, an inadequate range for discriminating coating performance. Modified procedures were attempted to resolve these problems, but results were not promising.

A related test that provided much improved force alignment and generally more robust test specimens was a double lap shear configuration (Fig. 6) that followed ASTM (2002) D3528-96. In this configuration, a single coupon encased on two sides by ice 0.125 in. (0.317 cm) thick was used, in-

stead of a coupon pair. The contact area between the ice and the coupon could be readily increased from 1 up to 3+ $in^2$. A preliminary test on 17 May evaluated the effect of fill depth and contact area on the load response of uncoated control coupons in double lap shear at a deformation rate of 0.002 in./min. Figure 7 depicts these coupons in aluminum holders with tape providing the mold for the chilled water.

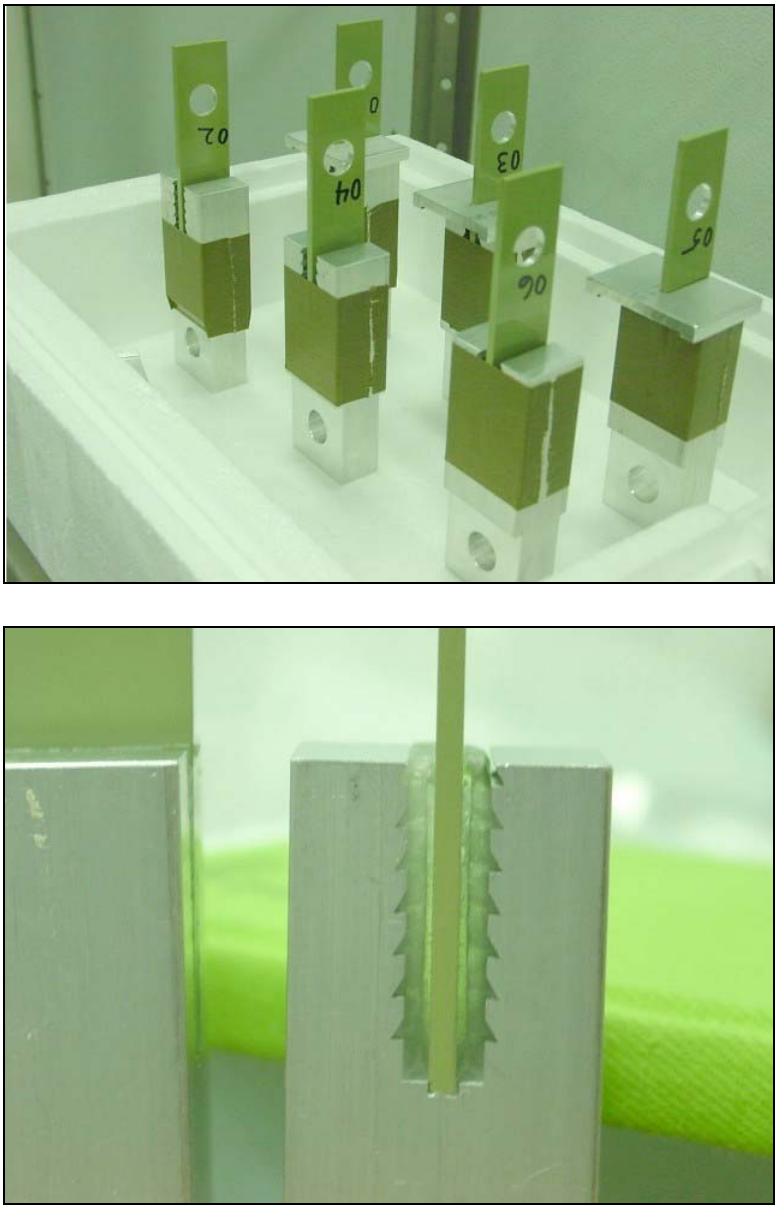

Figure 7. Double lap shear molds formed with tape (top). These molds are filled with water in a +1ºC coldroom. The sample caps (back row) hold the coupons in alignment during the freezing process. Close-up of double lap shear sample cooling in the coldroom after freezing in the cold box (bottom).

The load response patterns of these preliminary tests of uncoated coupons were consistent. The load increased linearly to a primary peak followed by a sharp load decrease at the initial ice failure. Then, successive load increases to secondary peaks, followed by abrupt decreases with ice fractures, repeated periodically. These tests followed intuition in that peak loads increased with the ice–coupon contact area. Maximum loads exceeding 1000 lbf provided the necessary range to discriminate coating performance.

Subsequent preliminary double lap shear tests on 24 May evaluated different holders and strain rates. The aluminum holder shown close-up in Figure 7 was selected for use, except that the downward slanting roughness elements were replaced by an equal number of upward slanting roughness elements. A low and constant deformation rate of 0.005 in./min was used for about the first 10 minutes of each test, followed by a 20× higher rate of 0.1 in./min until a total displacement of 0.5 in. was attained. Samples in the double lap test configuration were robust, with none being damaged during handling in the preliminary tests. There was no visible damage to the Koropon coupon surfaces as a result of the testing. On the basis of these positive results, the ice mitigation team decided to proceed with double lap shear testing of many candidate coating materials in what became the first of three test phases.

# 3 Sample Preparation and Test Protocols

Bracket temperatures obtained by NASA were used to design the temperature regime of the CRREL experiments. The NASA temperature data indicated maximum temperature decreases of 23–26°C/hr (41–47°F/hr) in response to cryogenic fuel loading. Most of the temperature decrease occurred over a 6-hour period at an average rate of 16–17°C/hr (29–31°F/hr). These measured temperatures continued to decrease over 8+ hours, asymptotically approaching a minimum surface temperature of –112°C (–170°F) at an overall average rate of 11–12°C/hr (20–22 °F/hr).

The CRREL experiments did not attempt to simulate prototype ice growth from vapor and condensate rundown, a source of potentially large variability. Instead ice was initially grown as strong and consistently as possible, and then subjected to temperature decreases comparable to those of the prototype bracket. Ice growth and temperature reduction procedures used in the double lap shear tests were identical to those used previously with the single lap shear tests. Sample preparation required a full day prior to the start of testing. Distilled, de-ionized, and de-aerated water was cooled to ~1°C and placed in sample molds that were also cooled to just above the freezing point. The samples were then placed in a cold box at variable but stable temperatures between –6 and –10°C (21 and 14°F), where ice growth occurred over a period of 4–5 hours. Figure 8a shows the filled holders placed onto a cold plate in the cold box, and samples being covered by a Styrofoam enclosure immediately after placement in the cold box, further regulating and stabilizing temperature (Fig. 8b). Following ice growth and cool down to the cold box temperature, samples were removed and placed in the cold room outside, and allowed to equilibrate to a temperature of about –18°C (0°F) for a period of 2 hours. Figure 7 (bottom) shows a sample that had been frozen in the cold box and is cooling further in the cold room.

Transport from the coldroom to the test chamber (Fig. 5) followed, where the samples were maintained at –20°C (–4°F) until the cool down immediately prior to testing. The desired temperature variation of the test chamber is programmed into the controller, which opens a valve and sends liquid nitrogen ($LN_2$) flowing through an insulated ¾-in. stainless steel flexible tube. Upon reaching the chamber, the nitrogen is dispersed

through a radiator. Flow of $LN_2$ continues until the desired chamber temperature is reached. The system then maintains this temperature by adjusting the flow of $LN_2$. A fan operates continuously to equalize the temperatures throughout the chamber.

a. Placing the samples.

b. Insulated cover to isolate the samples inside the cold box for maximum temperature stability.

Figure 8. Samples placed in the cold box for freezing and initial temperature reduction.

During cool down, the test chamber temperature decreased linearly over a period of 6 hours from –20°C to the desired bracket surface test temperature of –112°C, an average rate of 15.3°C/hr (28°F/hr). The chamber was then maintained at this temperature for 1 hour prior to testing, allowing time for sample and chamber temperatures to equilibrate and stabilize.

Samples were accessed for sequential testing through ports in the chamber door using the –250°C (–418°F) gloves attached to the ports (Fig. 5). This procedure eliminated any need to open the chamber door during testing which, at this temperature, would have introduced moisture and created frost in the system, used a much greater quantity of $LN_2$, and introduced a large temperature recovery time into the protocol. Three tanks of $LN_2$ were used during a normal test to achieve the desired temperature control. Following each test, the failed samples were routinely taken to a coldroom for inspection, correlation with test data, logging of characteristics, and photographs.

The temperature regimes of 20 and 21 June 2005, given in Figure 9, are typical of the patterns associated with sample freezing and subsequent temperature reduction. Samples were placed in the cold box just after 0800 on 21 June, and the heat of the samples raised the temperature under the insulating cover to almost –7°C. This maximum temperature was maintained for about 30 minutes, followed by an asymptotic temperature decrease over a 4-hour period. Sample freezing and temperature equilibration at –10°C were complete by 1300. Samples were removed from the cold box at 1420, as reflected in a temperature oscillation both under the cover and inside the cold box. Coldroom temperatures were not as stable as those of the cold box, oscillating ±1°C continuously about a mean of –15°C, with defrost cycles causing larger excursions just after 0800 and just before 1600. The test chamber temperature reduction for the samples prepared the previous day is also given in Figure 9. Cooling of the chamber for the test on 21 June began at 1420 on 20 June. The chamber attained the holding temperature of –20°C at 1520, and maintained that temperature until the linear temperature decrease began at 0320 on 21 June. A change of the $LN_2$ tank at 0700 briefly disturbed the temperature decrease, which then continued until the –112°C test temperature was attained at 0900 on June 21. Stable temperature of the test chamber was then maintained until testing began after 1000 and throughout the testing. A second $LN_2$ tank change and corresponding temperature fluctuation occurred during the testing.

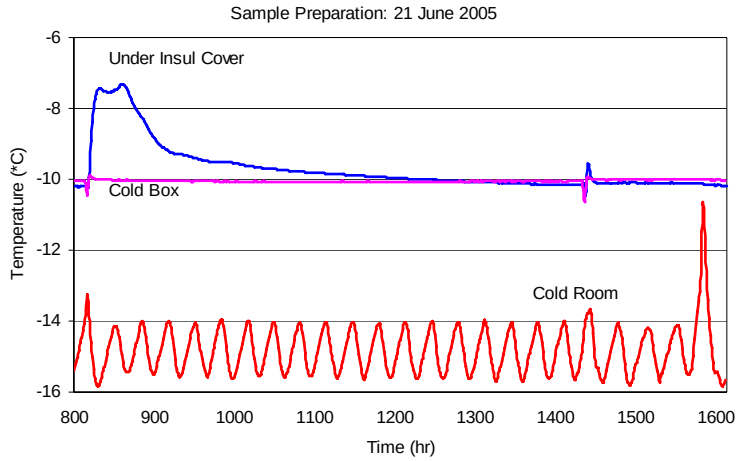


a. Sample ice growth under the insulated cover inside the cold box (samples removed at 1420), the cold box itself, and the larger coldroom outside.

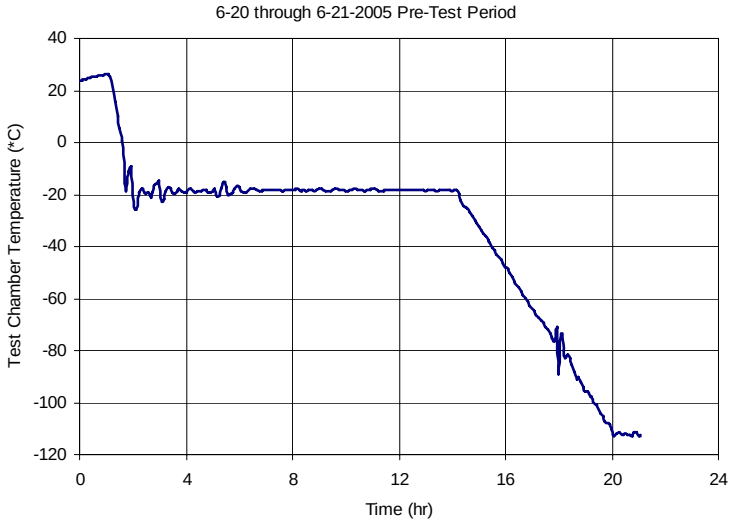


b. Test chamber with temperature decrease beginning at 1420 with initial –20ºC attained at 1520 on 20 June. The linear temperature decrease begins at 0320 on 21 June, an $LN_2$ tank is changed at 0700, arrival at –112ºC at 0900, and test initiation after 1000.

Figure 9. Typical temperature regimes.

# 4 Methods of Data Analysis

Load data were recorded several times per second during each test. From these data, the peak load and total work were obtained and reported. Peak load is an instantaneous measure that can occur at either strain rate. Conversely, total work is an integrated measure of load applied to the sample through distance. Because of the basic difference between instantaneous and integrated values, both measures provide important quantitative information concerning ice adhesion. However, these measures are not adequate to fully characterize the load–time response throughout a double lap shear test.

Work is directly related to strain rate, and the high strain rate segment of a test dominates the total work applied to a sample. Because of this strain rate dependence, work was recomputed as a pair of integrated values, corresponding to both individual strain rates. These work measures quantify strain rate effects and are not subject to the dominance of high strain, like total work. Another potential problem with the work measures is the effect of variable load application time in different tests altering the work when the adhesion is unchanged. To determine whether this problem exists and correct for it, a pair of power measures was obtained to normalize the work at each strain rate to corresponding rates of work.

A final characteristic of the load–time response that should be quantified is the short-term variation in load or "stick–slip" of a sample. The basic character of these short-term variations can change between controls and coated samples, between coatings, or between strain rates of a single coating. An automated measure that captures the short-term variability of the load is the standard deviation from the mean over short time intervals. An average of these values through time by strain rate provides a pair of stick–slip measures for each test.

# 5 Overview of Test Program

The decision to proceed with double lap shear testing was followed with a testing program that evolved into three primary phases. The first phase of this program quantitatively evaluated the performance of a wide range of candidate coating materials, while the second phase focused on variations of the mix to enhance the durability of the optimal phase 1 coating, and the third phase evaluated handling, application, resistance to weathering by water, and durability of the optimal coating.

## Phase 1

DeWeese et al. (2006) did preliminary testing on a large number of coating materials to determine the relative effectiveness of these materials to reduce the adhesive strength of ice to flat, epoxy-coated aluminum panels subject to impact. Following these tests they concluded that Rain-X and Braycote 601EF consistently reduced the adhesive strength of ice, and that Rain-X provided the more repeatable results. The composition of Rain-X, according to the MSDS, is as follows: ethanol/SD alcohol 40 86%; isopropanol 4%; ethyl sulfate 1%; polydimethylsiloxanes (silicon oil) <9%; silicic acid (H4SiO4), tetraethyl ester, hydrolysis products with chlorotrimethylsilane <9%; and siloxanes and silicones, di-Me, hydroxy-terminated <9%. The recommended coatings for further testing were, in order, Rain-X mixed with maximum MP-55, Rain-X mixed with typical MP-55, Braycote 601EF mixed with maximum MP-55, Braycote mixed with maximum UF-8TA, and Braycote mixed with typical UF-8TA. All the Braycote mixtures were applied to Scotch Brite abraded epoxy surfaces. The maximum designation of the mixes means almost equal weights of binder (51.4%) and filler (48.6%), and typical indicates less MP-55 or UF-8TA filler (41.4%) and more binder (58.6% by weight). The typical mixture provides good workability while including a large quantity of filler, and the maximum mix sacrifices some workability to include additional filler.

UF-8TA is an ultra-fine polytetrafluoroethylene (PTFE) powder with an average agglomerated particle size of 4.0 μm, average particle size of 0.3 μm, and component particle sizes as small as 200 nm (0.2 μm). The density of UF-8TA is 450 g/L. It is specially treated for compatibility and made for release applications where superior dispersion is needed. Improved properties over standard PTFE include extremely good release,

chemical inertness to all industrial chemicals and solvents, wide range of service temperatures from –240 to 250°C (–400 to 482°F), low friction, and excellent non-stick properties. In comparison, MP-55 is white, fine-particle PTFE micro-powder with an average particle size of 4.0 μm, minimum particle size of 0.2 μm, and density of 300 g/L. It is used as an additive in several applications, including dry film lubricants and coatings. The difference in bulk density among these powders indicates fundamental differences in particle size distribution that may affect the reduction in ice adhesion achieved.

Following the input of DeWeese et al. (2006), a phase 1 test schedule was developed and is given in Table 1 with the following coating material abbreviations:

- **LL** is a **l**ight or thin coating of NAPA **l**ithium grease, and no surface abrading.
- **LM** is a **m**oderate thickness coating of NAPA **l**ithium grease, and no surface abrading.
- **LTN** is white **l**ithium grease with **T**eflon (Champion spray), and **n**o surface abrading.
- **LGN** is NAPA **l**ithium grease with 27% by weight Knox **g**elatin added, and **n**o surface abrading.
- **LNN** is NAPA **l**ithium grease with 5.5% by weight **n**anogel added, and **n**o surface abrading.
- **BM** is **B**raycote 601EF with the **m**aximum amount of MP-55 (powdered Teflon) added and applied to Scotch Brite abraded coupon surfaces.
- **BMN** is **B**raycote 601EF with the **m**aximum amount of MP-55 added, and **n**o coupon surface abrading.
- **BUM** is **B**raycote 601EF with the **m**aximum amount of **U**F-8TA (ultra fine powdered Teflon) added and applied to Scotch Brite abraded coupon surfaces.
- **BUT** is **B**raycote 601EF with the **t**ypical amount of **U**F-8TA added and applied to Scotch Brite abraded coupon surfaces.
- **UNC** 8K, 4K, 1/4K, and 1K are four functionally endcapped, fluorocarbon-based oligomers that are crosslinked with isocyanates, developed and applied at the **U**niversity of **N**orth **C**arolina.
- **RXM** is **R**ain-**X** with the **m**aximum amount of MP-55 added, and no surface abrading.

- **RXT** is **R**ain-**X** with the **t**ypical amount of MP-55 added, and no surface abrading.

Table 1. Phase 1 coating evaluation test series.

| Test Date (2005) | Controls | Coating 1 | Coating 2 | Coating 3 |
|---|---|---|---|---|
| 17 May | 15-20 | Investigate alternative fill depths | | |
| 24 May | 21-29 | Investigate alternate coupon holders and strain rates | | |
| 26 May | 30-33 | LL 1-4 | LM 1-4 | |
| 7 June | 34-46 | Control sample only test | | |
| 8 June | 47-48 | RXM 1-10 (cy 1) | | |
| 9 June | 49-50 | RXT 1-10 (cy 1) | | |
| 10 June | 51-52 | BM 1-10 | | |
| 14 June | 53-54 | BUM 1-10 | | |
| 15 June | 55-56 | BUT 1-10 | | |
| 17 June | 57-58 | RXM 2,4,5,7,8 (cy 2) | RXT 1,3,4,7,9 (cy 2) | |
| 21 June | 59-60 | BMN 1-4 | LTN 1-5 | |
| 22 June | 61-62 | LGN 1-4 | LNN 1-4 | |
| 1 Sept | 63-64 | UNC 8K 1-2 | UNC 4K 1-2 | |
| 21 October | 75-76 | RXM 2,8 (cy 3) | UNC 1/4K 1-2 | UNC 1K 1 |

The RXM, RXT, BM/BMN, BUM, and BUT coatings were mixed at NASA-MSFC and shipped to CRREL. From 6–9 June 2005, E. Weiser, T. St. Clair, R. Cano, and T. Smith applied these coatings and also applied the LL, LM, and LTN coatings, and mixed and applied the LGN, and LNN coatings. Epoxy coated aluminum specimens received from MSFC were wiped clean with isopropyl alcohol (IPA) and used as received. Selected specimens were lightly abraded by hand parallel to the testing direction with a Scotch Brite pad. All the coatings except LTN were applied using translucent, skin-colored, laboratory latex gloves to produce an even coating. LTN was sprayed on from a distance of approximately 8 to 10 in. to uniformly cover the test coupons. The RXM and RXT coating materials supplied were each mixed with 1 mL of IPA prior to application, and coatings that resulted had variable thickness, characterized from "thick" to "thin." BM and BMN coupons had uniform thickness, while BUM and BUT samples had caking or pilling of the ultra-fine Teflon during application. The LTN spray produced an "orange peel" effect on the coated surface, LGN had pilling during application, which produced a grainy coating with some thickness variability, and LNN produced minor pilling during application. Rain-X, Braycote, and lithium grease coated coupons are pictured in Figure 10. J. DeSimone and C. Wood of the University of North Carolina supplied UNC coated coupons directly to CRREL for testing.

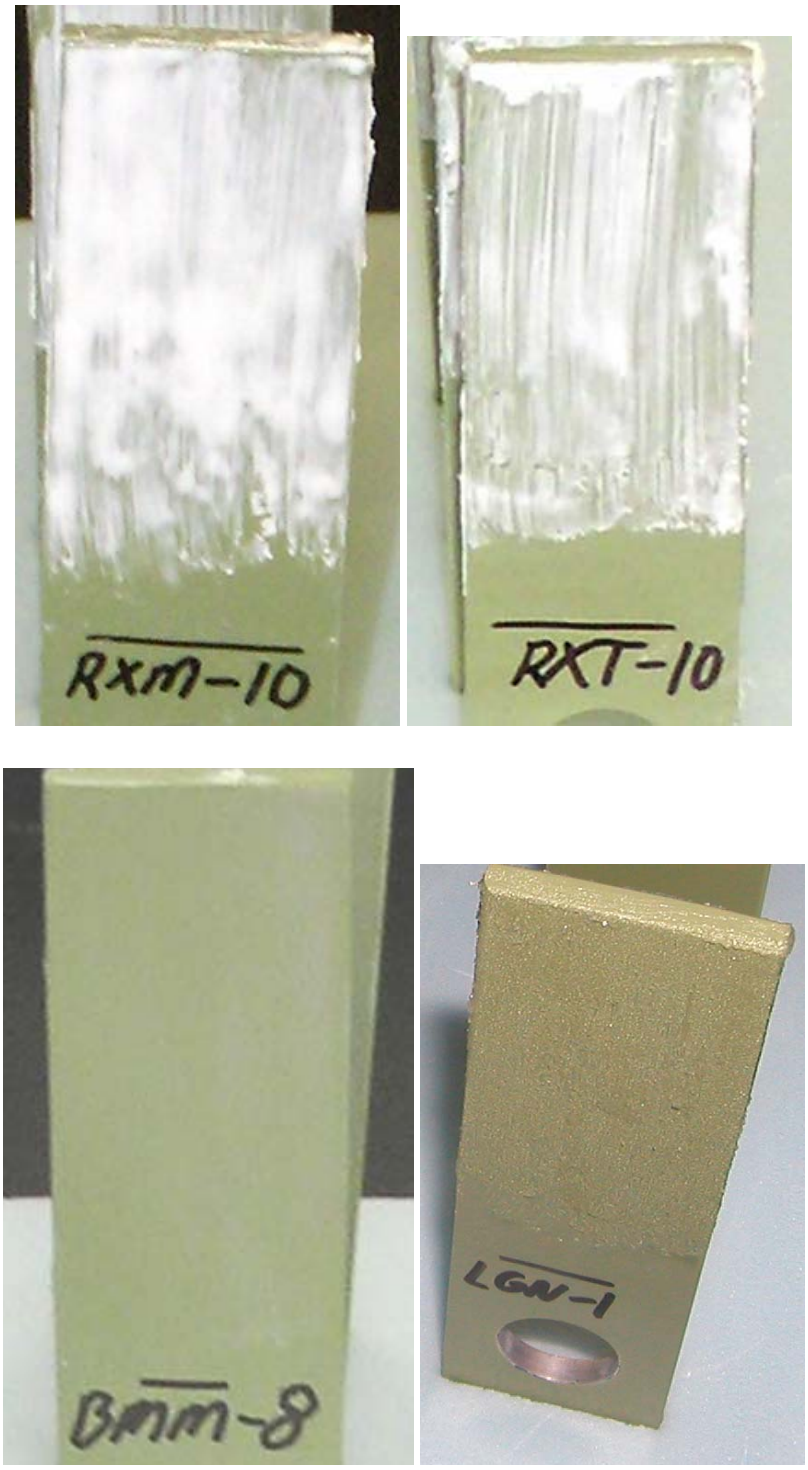


Figure 10. Selected phase 1 coated coupons prior to testing (clockwise from top left): Rain-X with maximum MP-55, Rain-X with typical MP-55, NAPA lithium grease with Knox gelatin, and Braycote 601EF with maximum MP-55 on an abraded surface.

## Phase 2

Four batches of coating materials were prepared by E. Martinez at CRREL on 29 September 2005. The compositions of these mixtures are detailed in Table 2, where: 100-0 is 100% Rain-X, with 0% DF 1040 silicone fluid, and the maximum amount of MP55 powdered Teflon added; 97.5-2.5 is 97.5% Rain-X, with 2.5% DF 1040, and the maximum amount of MP55; 95-5 is 95% Rain-X, with 5% DF 1040, and the maximum amount of MP55; and 90-10 is 90% Rain-X, with 10% DF 1040, and the maximum amount of MP55. These formulations will often be denoted by the percentage of DF 1040 in the mixture as 0, 2.5, 5, and 10. In all mixtures the amount of Rain-X was diminished in weight to accommodate the addition of the DF 1040, while the amount of MP55 was held constant.

Table 2. Phase 2 coating mixtures by weight.

| Formulation | Component | Target % by wt. (g) | Target wt. (g) | Actual wt. (g) |
|---|---|---|---|---|
| 100-0 | Rain-X | 51.5 | 25.75 | 25.77 |
| | DF 1040 | 0.0 | 0.0 | 0.0 |
| | MP-55 | 48.5 | 24.25 | 24.24 |
| 97.5-2.5 | Rain-X | 40.0 | 24.5 | 24.5 |
| | DF 1040 | 2.5 | 1.25 | 1.24 |
| | MP-55 | 48.5 | 24.25 | 24.23 |
| 95-5 | Rain-X | 46.5 | 23.25 | 23.28 |
| | DF 1040 | 5.0 | 2.5 | 2.5 |
| | MP-55 | 48.5 | 24.25 | 24.26 |
| 90-10 | Rain-X | 41.5 | 20.75 | 20.80 |
| | DF 1040 | 10.0 | 5.0 | 5.1 |
| | MP-55 | 48.5 | 24.25 | 24.27 |

The mixing procedure for 50-g batches (Table 2) of these coatings began by combining the Rain-X and DF-1040 liquids in a glass container and mixing for 100 strokes using the square edge of a small lab spatula. The MP-55 was then weighed and added, and mixing continued for 300 additional strokes. Every 100 mixing strokes during this procedure, the sides and bottom were scraped, and then mixing continued. The contents of the glass jar were then transferred into a mortar and mixed with a pestle for 100 strokes. After 100 strokes, the sides and bottom of the mortar and the pestle were scraped with a small lab spatula to push the mix back to the bottom. This procedure was repeated for a total of 300 mixing strokes. Firm and gentle pressure with a rotating grinding motion of the pestle was applied to the mixture against the sides of the mortar. The final mixture

was transferred into a clean glass bottle using the spatula, and the lid of the bottle was tightened to minimize evaporative loss of the Rain-X solvent. This blending and mixing procedure produced consistency between the batches, especially important for a hand procedure.

Simultaneously, A. St. Clair and T. St. Clair cleaned the epoxy coated aluminum test coupons with IPA; drying them in air; and dip coating them in a beaker of the organosilicate–organotitanate primer, DC 1200. The Koropon surfaces were not abraded. The primer was a pink/orange fluorescent liquid that dried to a pinkish-white powder. Of particular interest was that four of the coupons exhibited defects in the epoxy coating that was only visible after dipping them into the DC 1200. These four coupons were discarded. The primed coupons were allowed to air dry in a chemical hood for about 1/2 hour prior to the start of coating. There was very little delay between the preparation of the coating mixtures and the actual coating of the coupons. The 10% mixture was used almost immediately after it was prepared, while the 2.5% mix had the longest lag time of about 30 minutes between mixing and coating.

All the mixes were applied using latex laboratory gloves. Care was taken to make only a single, rapid pass over the surfaces and edges of the coupons because subsequent passes resulted in damage to the rapidly drying initial coating. The 0% mix with no DF 1040 had a very dry consistency, making it the most difficult to apply. With increasing DF 1040, the application became easier. About 10% of the time, lumps in the mixtures were inadvertently applied to the panels. These were carefully removed with the fingertip and more coating mixture was lightly dabbed onto that area. Sample 9 of the 2.5% mix and Sample 6 of the 5% mix had large coated areas that contained clumps of dry Teflon powder. All the sample groups are depicted in Figure 11 following the coating application. The subsequent phase 2 test dates with corresponding mixes and coupons tested are presented in Table 3. The 2.5% coupons were kept in reserve and were not tested.

Figure 11. Phase 2 coated coupons prior to testing: Left group has 10% DF1040, second group has 5% DF1040, third group has 2.5% DF1040, and far right group has 0% DF1040.

Table 3. Phase 2 coating durability evaluation test series.

| Date (2005) | Controls | Coating 100-0 | Coating 95-5 | Coating 95-5 | Coating 90-10 |
|---|---|---|---|---|---|
| 4 October | 65-66 | | 1-5 (cy 1) | | 1-5 (cy 1) |
| 6 October | 67-68 | 1-5 (cy 1) | | | 1-5 (cy 2) |
| 11 October | 69-70 | 1-5 (cy 2) | 2-5 (cy 2) | 6 (cy 1) | |
| 13 October | 71-72 | | 2-5 (cy 3) | 6 (cy 2) | 1-5 (cy 3) |
| 17 October | 73-74 | 1-5 (cy 3) | 3,4 (cy 4) | 6 (cy 3) | 1,4 (cy 4) |
| 21 October | 75-76 | 2,3,4 (cy 4) | 2 (cy 4) | | 5 (cy 4) |

## Phase 3

R. Cano, E. Weiser, and T. St.Clair prepared coating materials on 3 November 2005 using Rain-X and MP-55 maximum with the same recipe used for the 0% mix in Phase 2. However, several variations in procedure were used, and results will be compared in these tests. The RM coating was mixed with a spatula, and the RP coating was mixed with a mortar and pestle. During the mixing of Rain-X with MP55, agglomerations of MP55 always form. This problem occurs whether the materials are stirred with a spatula or mixed with a mortar and pestle and becomes obvious when the mixture is applied to the coupons. The RD coating was also mixed with a mortar and pestle but was allowed to dry out with the Rain-X solvent evaporating. After drying, IPA was added with additional mixing in the mortar and pestle, providing the RD coating a more even texture than the RM and RP mixes and a very fine granular consistency. All coupon coat-

ings were applied using latex laboratory gloves, as before, and the Koropon surfaces were not abraded. Of this group of mixes, the RD coating was the easiest to apply. The RW samples, using the RP material, were allowed to dry and cure before being exposed to a forceful water stream (Fig. 12), which did not change the visual appearance of the coated coupons. Half of the coupons in the RP, RM, and RD groups were left untouched after application and curing, and are denoted as "a" sample subgroups RM(a), RP(a), and RD(a). The remaining coupons were wiped off with laboratory wipes after curing (Fig. 13) and are called "b" subgroups: RM(b), RP(b), and RD(b). The cure time of the RD coating was only about 30 minutes prior to wiping, much shorter than the 1.5-hour cure of the RM, RP, and RW coatings. The phase 3 coating preparation and handling, application, resistance to weathering by water, and durability testing program is presented in Table 4.

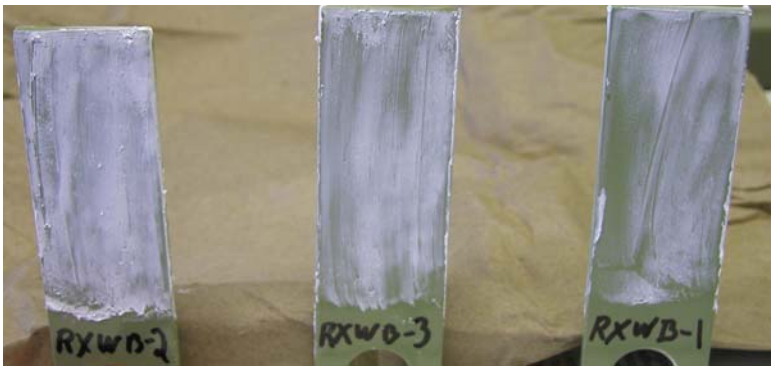


a. Prior to water stream exposure.

b. During water stream exposure.

Figure 12. Phase 3 RW coupons prior to and following exposure to a water stream.

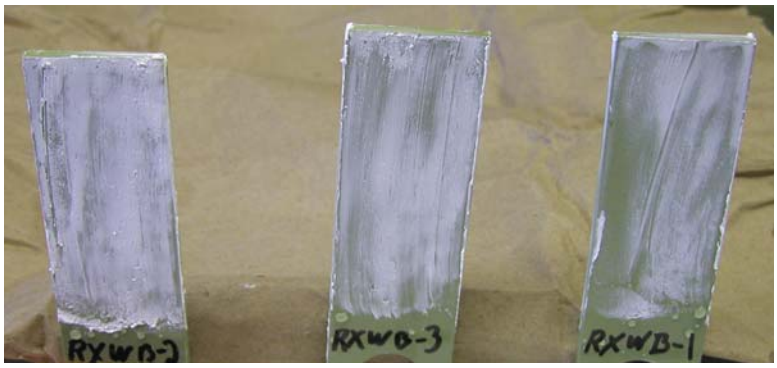


c. After exposure to water stream.

Figure 12 (cont'd). Phase 3 RW coupons prior to and following exposure to a water stream.

Table 4. Phase 3 optimal coating (Rain-X – MP-55) evaluation test series.

| Date 2005 | Controls | Applied | Applied andWiped Off | Applied and Water Stream |
|---|---|---|---|---|
| 15 November | 77-78 | RM 1-5 (cy 1) | RM 8-12 (cy 1) | |
| 16 November | 79-80 | RP 1-5 (cy 1) | RP 8-12 (cy 1) | |
| 17 November | 81-82 | RD 1-5 (cy 1) | RD 8-12 (cy 1) | RW 1-3 (cy 1) |
| 29 November | 83-84 | RM 1-5 (cy 2) | RM 8-12 (cy 2) | |
| 30 November | 85-86 | RP 1-5 (cy 2) | RP 8-12 (cy 2) | |
| 6 December | 87-88 | RD 1-5 (cy 2) | RD 9,11 (cy 2) | RW 1-3 (cy 2) |
| 7 December | 89-90 | RM 1-5 (cy 3) | RM 8-12 (cy 3) | |
| 8 December | 91-92 | RP 1-5 (cy 3) | RP 8-12 (cy 3) | |
| 9 December | 93-94 | RD 1-5 (cy 3) | RD 9,11 (cy 3) | RW 1-3 (cy 3) |


a. RM, RP, RD, and RW coupons after coating application.

Figure 13. Phase 3 coupons after coating both with and without wiping.

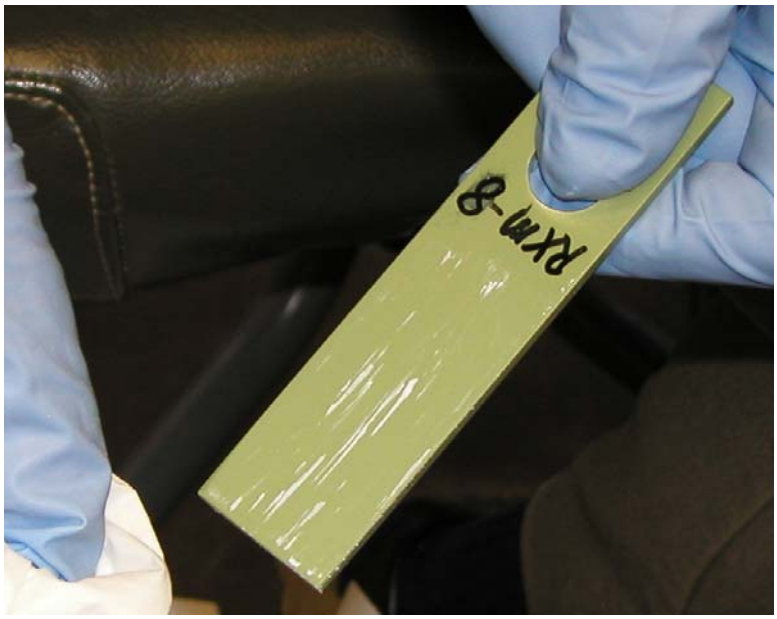


b. Wiping off coating after curing.

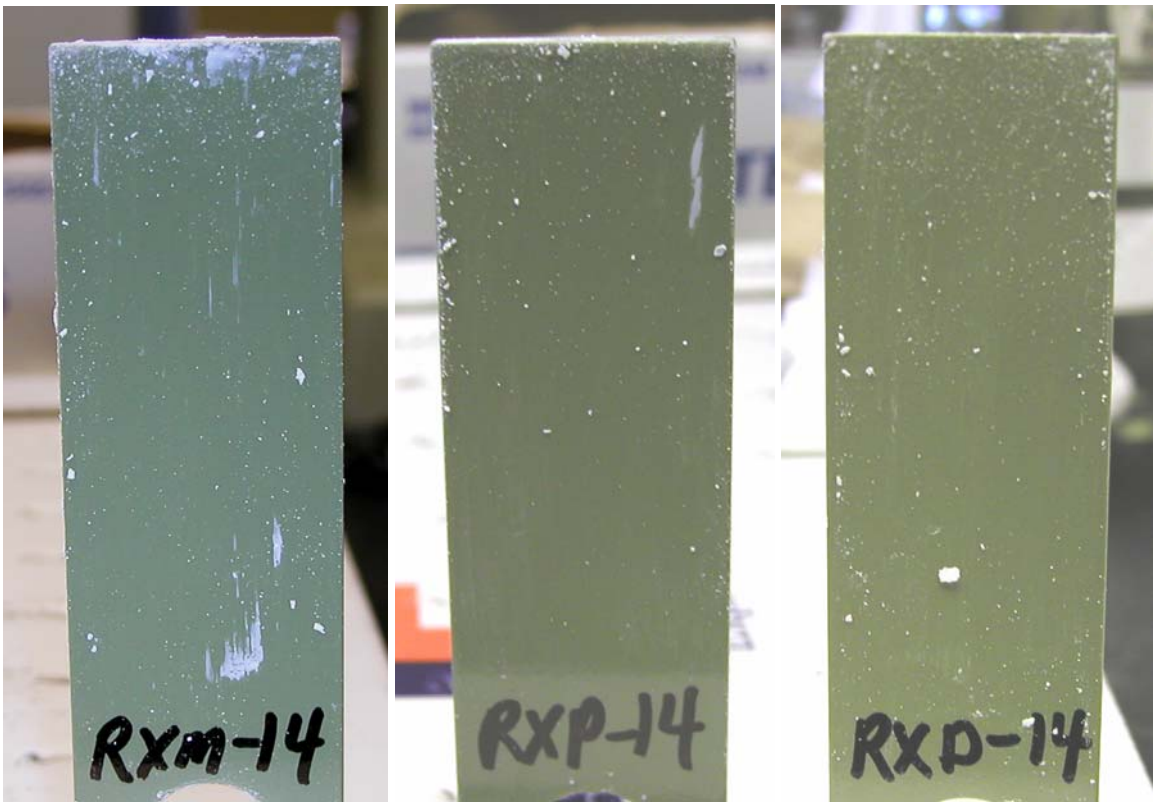


c. RM, RP, and RD coupons after wiping.

Figure 13 (cont'd). Phase 3 coupons after coating both with and without wiping.

# 6 Phase 1 Test Results

The phase 1 sample coupons tested fall into five primary groups: uncoated controls, lithium grease coated, Braycote coated, UNC coated, and Rain-X coated.

## Controls

The control tests were characterized by a series of audible ice fractures. The load typically increased linearly with time until a primary ice fracture occurred, greatly reducing the load. Subsequent linear load increases would be followed by subsequent fractures and sharply reduced load, producing a periodic "saw-tooth" pattern. The high strain rate later in the test served to accelerate the ice fracture process. The load–time and load–displacement responses of a particularly strong control from a test on 7 June 2005 are given in Figure 14. The diminishing amplitude of the load and scale of the saw-tooth with displacement and cumulative damage to the sample are evident. The change in strain rate at 9.5 minutes in this test, EP-46, greatly shortened the cycle of ice fracture and load recovery (Fig. 14). Post-test evaluation revealed extensively fractured ice that remained strong enough to hold the coupon against the force applied by an observer. Ice adhering to the coupon after testing, termed ice collars, was common for control samples.

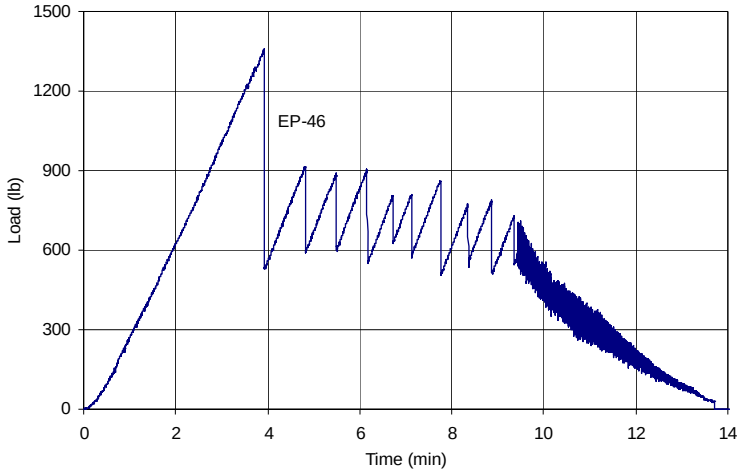


a. Load–time response.

Figure 14. Responses of control sample EP-46 in double lap shear testing.

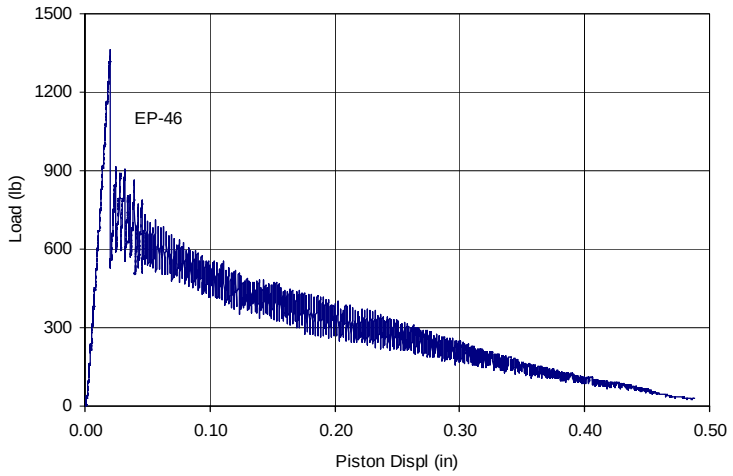


b. Force–displacement response.

Figure 14 (cont'd). Responses of control sample EP-46 in double lap shear testing.

## Lithium Grease

The lithium grease coated coupons without additives displayed extremely smooth load response with time. The load–time responses of representative samples from LM and LL sample groups are given in Figure 15. The LL coating displayed much lower peak loads and less total work than the LM coating, indicating that more lithium grease is not better at cryogenic temperatures. The high strain rate later in the tests applied load more rapidly and increased the slope. The LM peak loads increased significantly with the strain rate, but the LL peak loads did not. A post-test observer easily moved both the LL and LM coupons by hand.

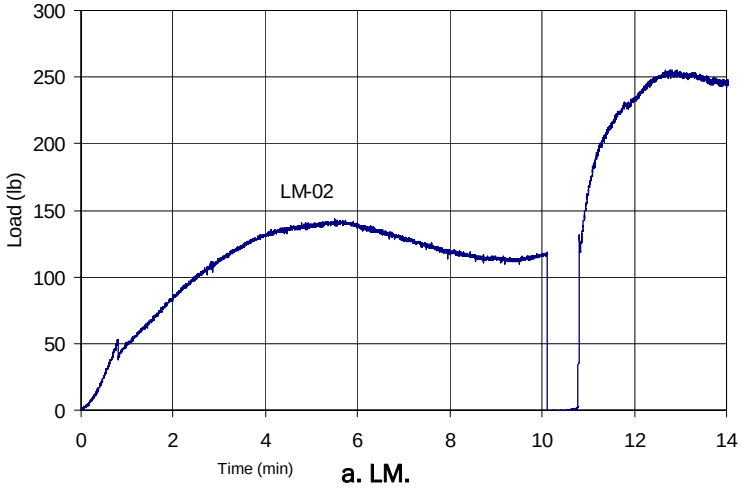


a. LM.

Figure 15. Load–time responses in double lap shear testing of representative lithium grease coated samples.

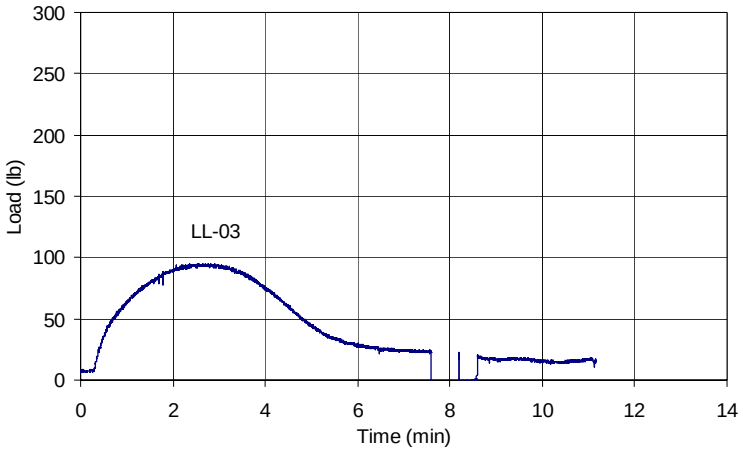


b. LL.

Figure 15 (cont'd). Load–time responses of representative lithium grease coated samples in double lap shear testing.

The additives mixed into the lithium grease varied in their effectiveness but did not produce a significant improvement in ice adhesion relative to the LL coating. Figure 16 gives the load–time response of representative samples of lithium grease with Teflon, with gelatin, and with nanogel additives. Lithium grease with Teflon produced peak loads that were only slightly reduced from those of the LM tests. Like LM, the LTN peak loads increased by about a factor of 2 at the high strain rate relative to peaks at the low strain rate. Lithium grease with gelatin produced the best overall results of this group. Peak loads at both strain rates were comparable, and almost exactly the same as the LL tests. Peak loads with nanogel added were intermediate to the others, as was the 25% increase in load at the high strain rate. A notable result of the LNN test series was the exceptionally consistent test results. The post-test hand pullout of LGN coupons was easy, that for LTN coupons was hard, and LNN coupons did not allow hand pullout.

The ice interface with the coupons was planar for all these coatings, with no evidence of damage to the ice, and no ice collars that adhered to lithium grease coated coupons. The smooth load responses and the sensitivity of LM, LTN, and LNN peak loads to strain rate indicate failure within the coating, a fundamental change in failure mechanism from that of the controls.

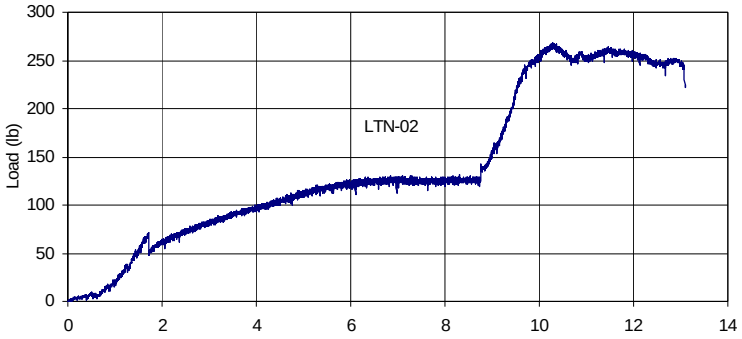


a. LTN (Teflon).

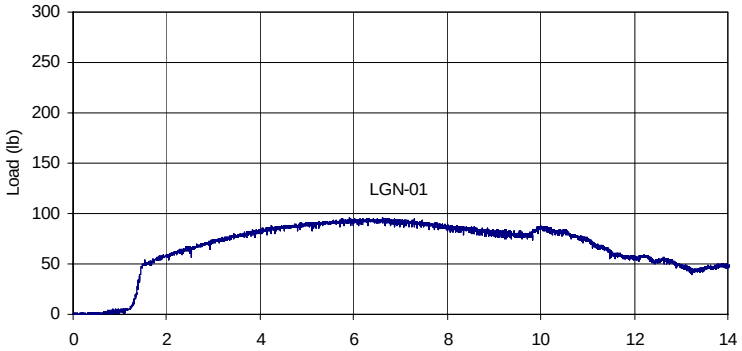


b. LGN (gelatin).

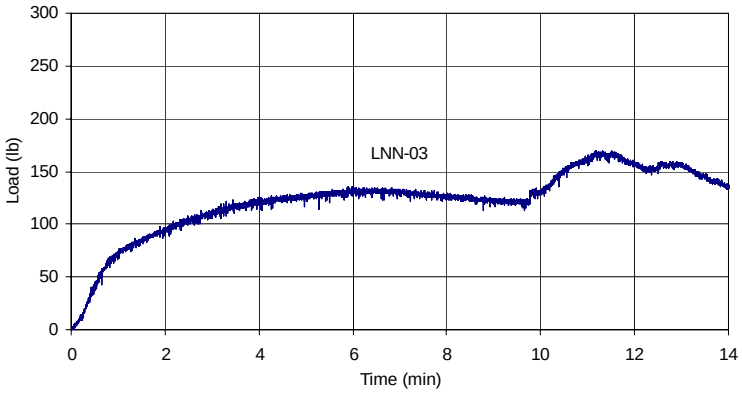


c. LNN (nanogel).

Figure 16. Load–time responses in double lap shear testing of representative lithium grease coated samples with additives.

## Braycote

Several variations of Braycote 601EF were tested in phase 1. The maximum amount of MP-55 Teflon was added to produce the BM and BMN coating that was applied to abraded and non-abraded coupon surfaces, re-

spectively. The maximum and typical quantities of UF-8TA Teflon were added to Braycote to produce the BUM and BUT coatings, and both were applied to abraded coupons. Representative load–time results for BM and BMN tests are given in Figure 17, and corresponding representative results for BUM and BUT tests are given in Figure 18. These figures show very similar shape and character of the load–time responses of all the Braycote samples. Almost all BM, BMN, and BUM samples responded with increased load when the strain rate was increased. The strain rate response of the BUT group, though generally similar, was less consistent. The BUM tests had the most consistent load–time and load–displacement response, and the most consistent peak loads at both strain rates. The peak load attained by and work applied to the BMN samples were significantly greater than those of the BM group, indicating an advantage to abrading the Koropon surface if Braycote is used to reduce ice adhesion. The performance of the BUM and BUT coatings were similar to each other, and showed improvement from the BM coating.

Following the tests there was significant coating material retained on all coupons. The planar ice interface was largely undamaged on most Braycote samples. Most BUM and BUT coupons did not retain ice collars, while the opposite was true for the BM coupons, and all BMN coupons had ice collars. The overall consistency and performance of the BUM coating indicate superiority of UF-8TA over MP-55 when mixed with Braycote. However, as UF-8TA was not mixed with other binders, their potential performance improvements remain unknown.

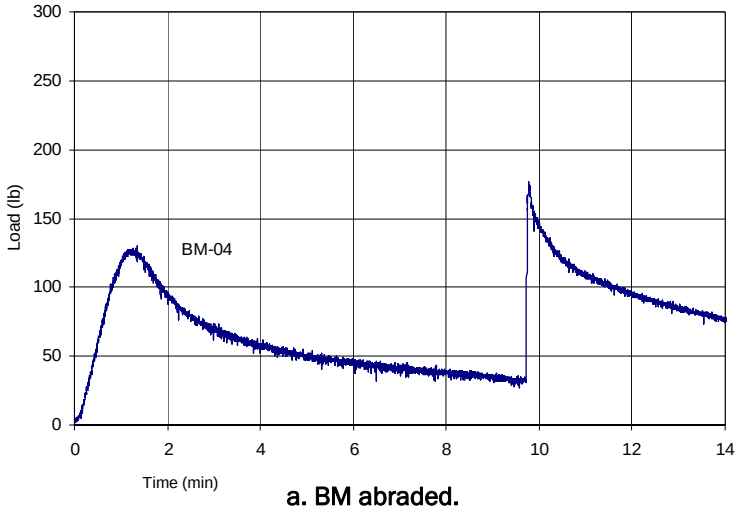


a. BM abraded.

Figure 17. Load–time responses in double lap shear testing of representative Braycote mixed with MP-55 coated coupons.

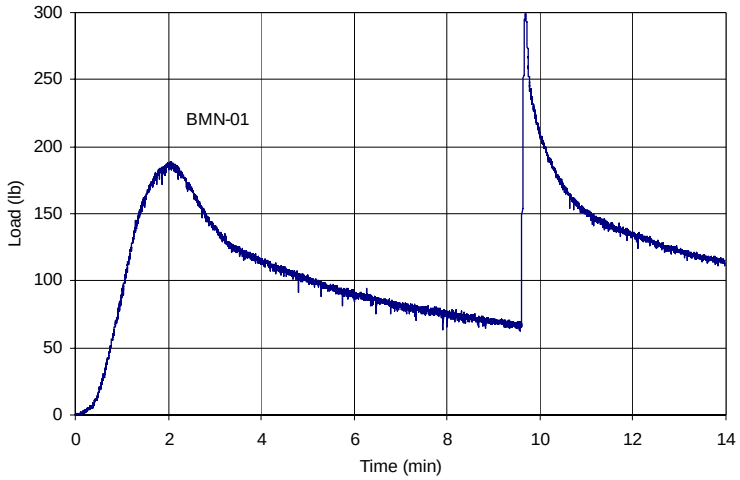


b. BMN unabraded.

Figure 17 (cont'd). Load–time responses of representative Braycote mixed with MP-55 coated coupons in double lap shear testing.

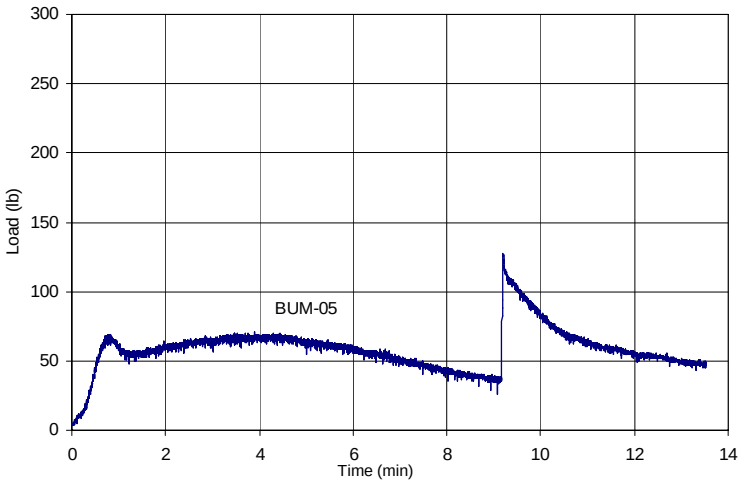


a. BUM maximum UF-8TA.

Figure 18. Load–time responses in double lap shear testing of representative Braycote mixed with UF-8TA coated on abraded coupons.

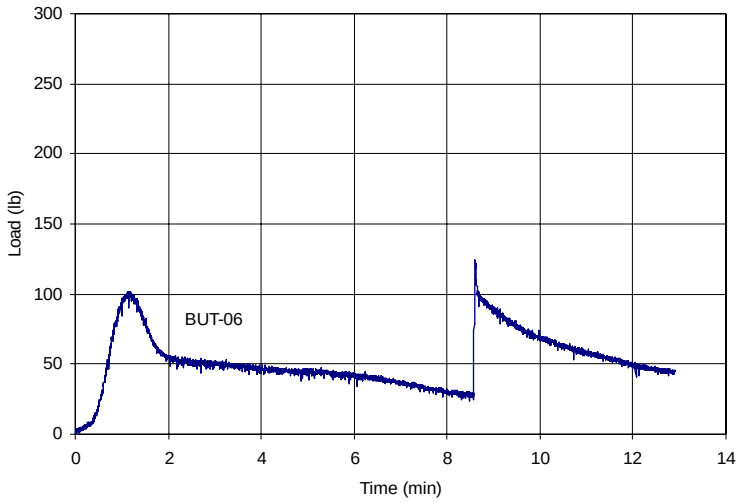


b. BUT typical UF-8TA.

Figure 18 (cont'd). Load–time responses of representative Braycote mixed with UF-8TA coated on abraded coupons in double lap shear testing.

## UNC Coatings

UNC provided seven coated samples for double lap shear testing. Load–time data for the 8K and 4K samples are given in Figure 19, and the 1/4K and 1K results are given in Figure 20. Peak load and total work for this entire group of samples are compared in Table 5. The 8K load-time data with a high initial peak followed by a saw-tooth and finally decaying loads at the high strain rate closely resembled the signature of the controls. The load–time characteristics of the 4K coating differed between the two samples tested, and also differed from the 8K signatures. The 4K peak-load and total work were significantly reduced relative to the controls, providing the maximum reduction in adhesive strength of this group. The 1/4K coating was nearly as effective as the 4K coating, with comparable total work. The load–time signature of both 1/4K samples shared common characteristics. Finally, the data for the 1K coating indicate less effectiveness than both the 4K and 1/4K coatings, resembling load–time, peak load, and total work of the 8K coating. Post-test analysis revealed that the 8K ice samples were totally destroyed with no residual strength, while the 4K and 1/4K ice sustained some fracturing. The 1K–ice sample was also significantly fractured during testing, placing it between the other two conditions. The UNC coatings as a group did not achieve the performance of the better coatings.

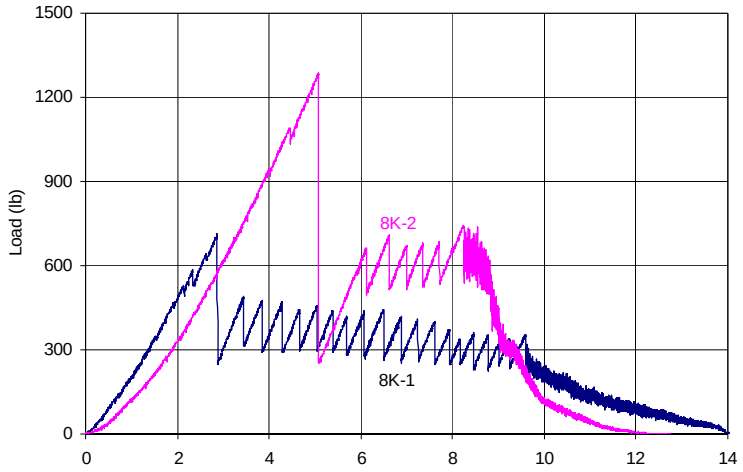


a. UNC 8K.

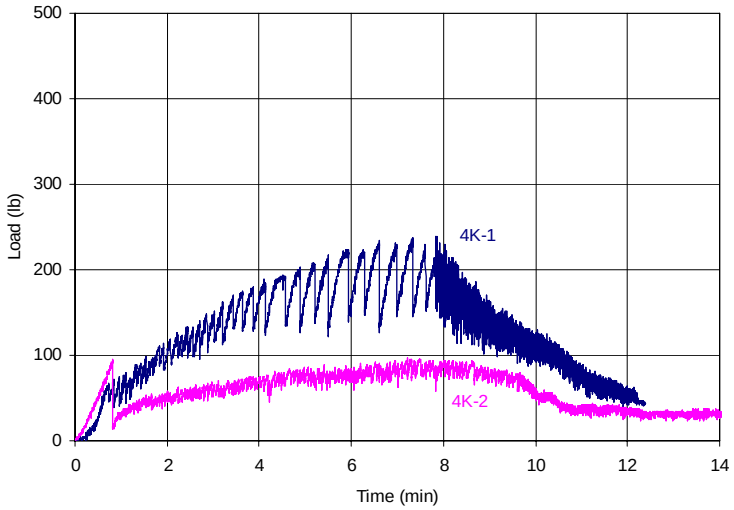


b. UNC 4K.

Figure 19. Load–time responses in double lap shear testing of UNC coated coupons.

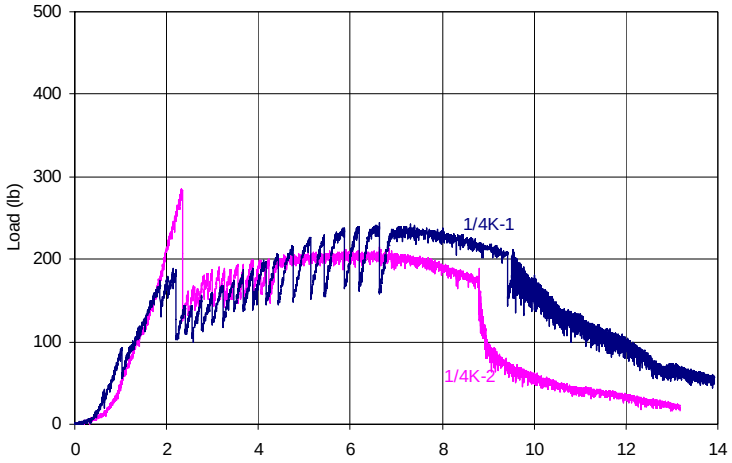


a. UNC 1/4K.

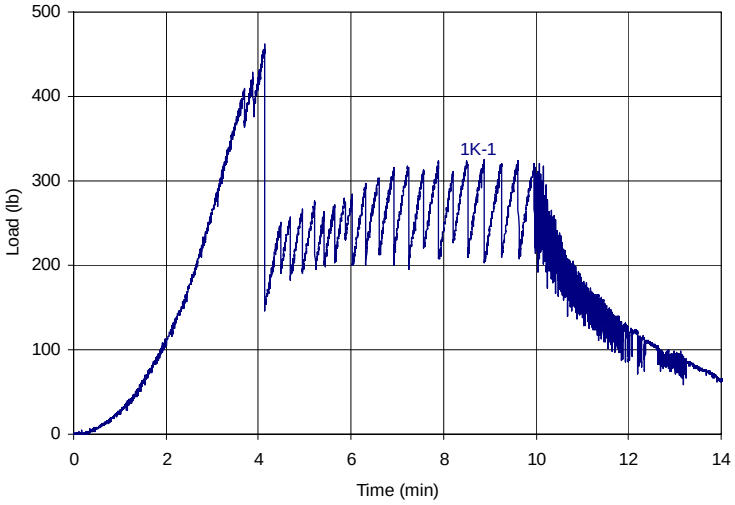


b. UNC 1K.

Figure 20. Load–time responses in double lap shear testing of additional UNC coated coupons.

Table 5. Summary of UNC coating results.

| Coupon | Peak Load (lb) | Total Work (lb-in.) |
|---|---|---|
| 8K–1 | 712 | 66 |
| 8K–2 | 1301 | 103 |
| 4K–1 | 255 | 55 |
| 4K–2 | 103 | 21 |
| 1/4K–1 | 247 | 55 |
| 1/4K–2 | 292 | 29 |
| 1K–1 | 465 | 69 |

## Rain-X

Rain-X was tested in two variations in phase 1, the first with the "maximum" amount of MP-55 in the mix (RXM), and the second with the "typical" amount (RXT). Representative load–time results for each group are given in Figure 21. The shape and character of the Rain-X load–time data were similar for samples in both groups, and overall performance was consistent and outstanding. Diminished load in response to increased strain rate was typical for both RXM and RXT samples. Post-test analysis revealed smooth ice at the interface with the coupon that did not show evidence of damage from testing, and coupons moved easily by hand. However, significant amounts of coating retained on the ice surface indicated both failure in the coating and the potential for loss of effectiveness with repeated cycles of ice formation and release. Peak load and total work data summaries for these cycle 1 tests are given in Table 6.

Five RXM and five RXT coupons that performed nearest the average for work and peak load in their respective groups were selected for a second cycle of testing. Representative load–time results for each group in cycle 2 are given in Figure 22. A change in shape of the load–time response can be noted between test cycles 1 and 2. The total work and peak load results of cycle 2 tests are also given in Table 6. The average total work for RXM samples remained constant, but variability in work increased. Average peak loads of RXM coated coupons increased, but peak load variability, as measured by the coefficient of variation, decreased. For RXT samples both peak load and average total work increased. Unlike cycle 1, RXM performance in cycle 2 was marginally better than RXT. Post-test sample analysis again had generally planar ice interfaces with no evidence of damage. Additional coating was retained on the ice surface, and very little coating remained visible on the coupons.

The best two coupons based on cycle 2 results, RXM-02 and -08, were retested a third time and their load–time results for cycle 3 are given in Figure 23. Total work and peak load recorded in these cycle 3 tests compare favorably to the cycle 1 and 2 results. Peak load and total work results, specific to these two coupons, are given over the 3 cycles in Figure 24. Peak load increased from cycle 1 to 2, but returned to the cycle 1 level in cycle 3. Total work diminished between cycles 1 and 2, and remained low in cycle 3. The question of RXM coating durability is not answered fully by these phase 1 results, but outstanding performance and indications of durability are promising.

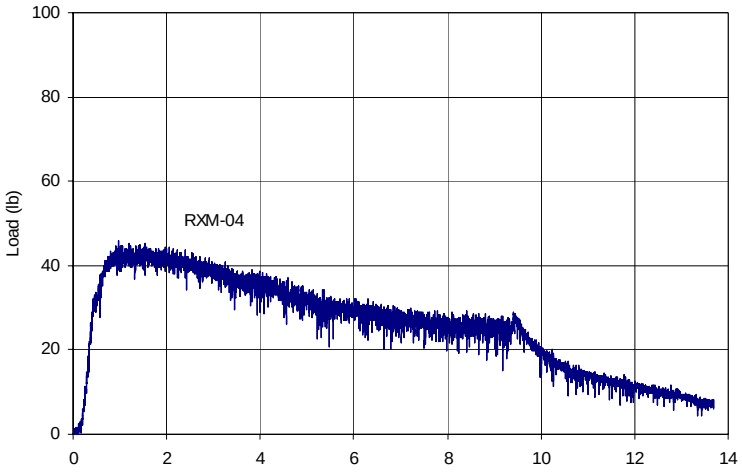


a. RXM maximum MP-55.

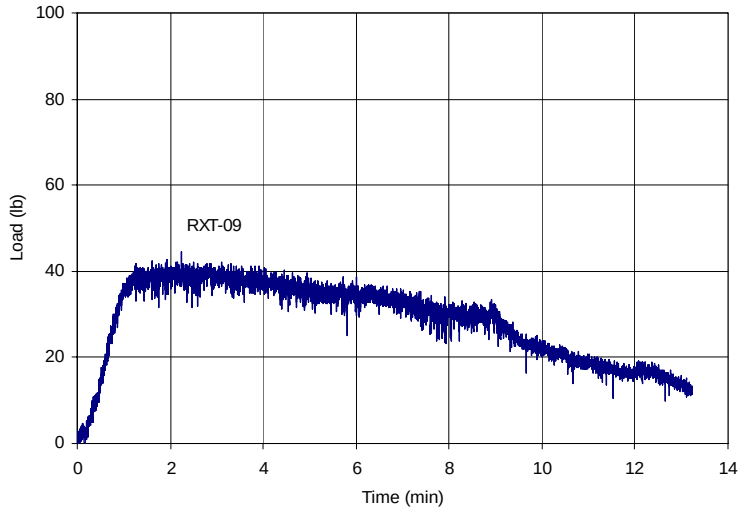


b. RXT typical MP-55.

Figure 21. Load–time responses in cycle 1 double lap shear testing of representative Rain-X mixed with MP-55 coated coupons.

Table 6. Durability results for RXM and RXT Phase 1 samples.

| Coating | Cycle | Total Work mean ± s.d. (lb-in.) | Range (lb-in.) | Peak Load mean ± s.d. (lb) | Range (lb) |
|---|---|---|---|---|---|
| RXM | 1 (10 samples) | 8.3 ± 2.6 | 5–14 | 51 ± 15 | 19–75 |
| | 2 (5 near ave) | 7.6 ± 4.4 | 4–16 | 87 ± 13 | 70–105 |
| | 3 (2 best) | 4.1 | 4–5 | 46 | 35–56 |
| RXT | 1 (10 samples) | 7.6 ± 1.9 | 4–11 | 43 ± 8 | 32–55 |
| | 2 (5 near avg.) | 10 ± 4.1 | 5–16 | 97 ± 16 | 78–125 |

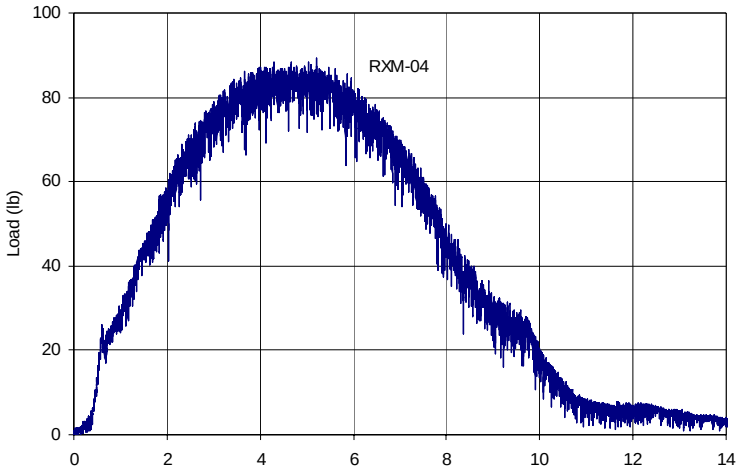


a. RXM maximum MP-55.

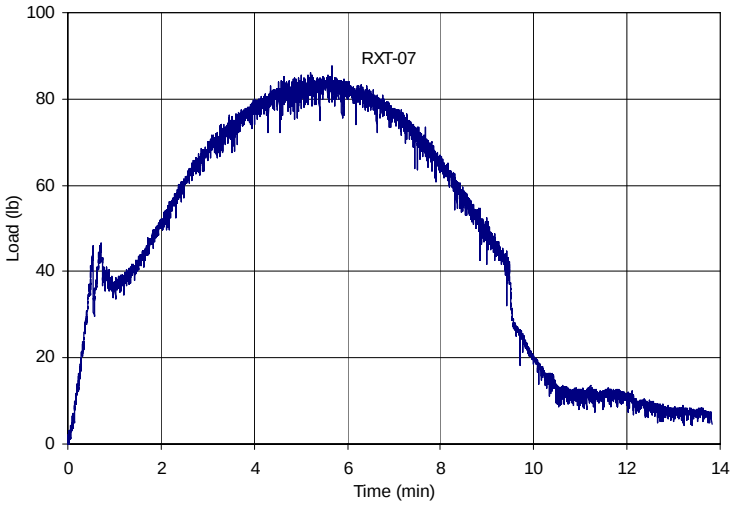


b. RXT typical MP-55.

Figure 22. Load–time responses in cycle 2 double lap shear testing of representative Rain-X mixed with MP-55 coated coupons.

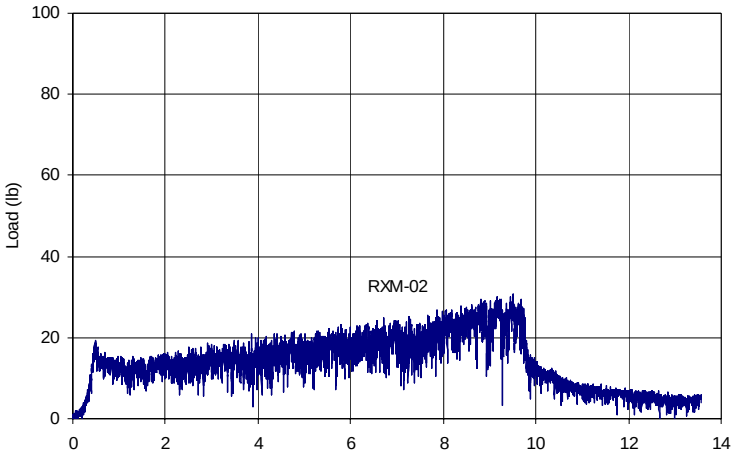


a. RXM-02.

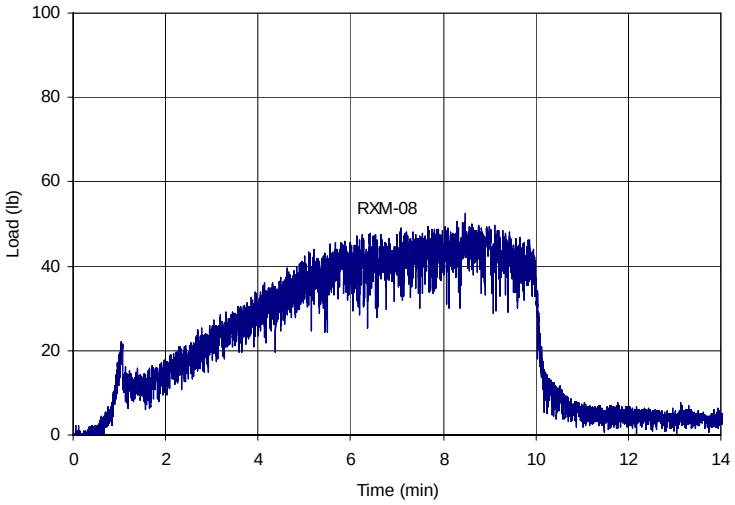


b. RXM-08.

Figure 23. Load–time responses in cycle 3 double lap shear testing of selected Rain-X mixed with MP-55 coated coupons.

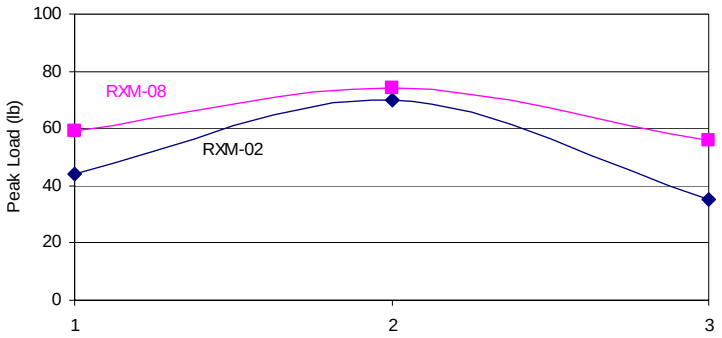


a. Peak load.

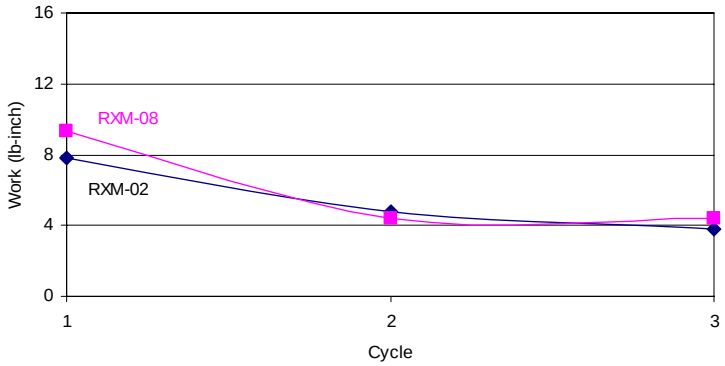


b. Total work.

Figure 24. Peak load and total work of RXM-02 and RXM-08 through three cycles of testing.

## Statistical Analysis of Peak Loads

A total of 14 coupons were available for use as controls in the CRREL phase 1 tests. The test procedure for evaluating each group of coated coupons required parallel testing of two controls to verify that no systematic errors were introduced in the results. With only 14 control coupons, repeat testing with most of these coupons was required. Coupons were selected for up to 4 cycles of repeat testing based on a lack of visual Koropon surface blemishes. An initial analysis is needed to compare the repeat test results for the controls and verify that there was no statistically significant change in performance of the Koropon surface with the repeat tests. Figure 25 provides a summary of the peak load measured for each coupon as a function of the number of times it was tested. A standard method to analyze these data is the ANOVA test to determine whether populations have statistically the same mean. However, ANOVA assumes that each popula-

tion is normally distributed, and sample sizes of 2, 7, 10, and 14 are not large enough to make conclusions about the nature of the probability density function (PDF). Therefore, a non-parametric method, the standard Kruskal-Wallis test (Siegel and Castellan 1988, Zar 1999), was used instead. The results of this test show that at the 95% confidence level ($\alpha$ = 0.05) the null hypothesis, that the means of all of the populations are the same, is true ($p = 0.147 > 0.05 = \alpha$).

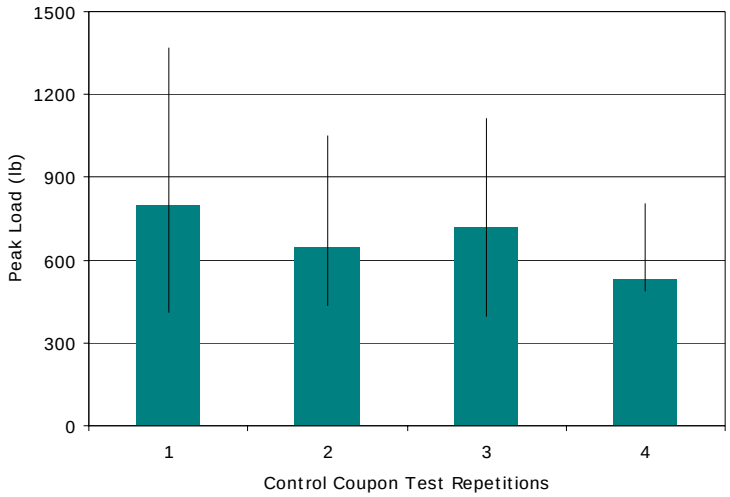


Figure 25. Summary plot of control coupon test repetitions. The x-axis indicates the number of times a coupon was tested; the height of each bar represents the median peak load of the population, while the error bar indicates the corresponding minimum and maximum.

Having established that the control coupons did not significantly degrade when subjected to repeat testing, the coated samples can now be compared to the controls. Peak load data for all phase 1 test series are summarized in Figure 26. Each bar represents the median of the series, and the error bars depict the corresponding minimum and maximum peak loads. The null hypothesis of the Kruskal-Wallis test in this case is that the means of all the coatings are the same as that of the control. The results of this analysis show that the null hypothesis is generally false. Only the UNC-8K coating has peak loads that are the same as those of the control. All other coatings have statistically significant lower peak loads, at the 95% significance level, than those of the controls. The Rain-X MP-55 coating performed better in cycle 1 than all of the other coatings evaluated (Fig. 26), but there was no statistical difference between the typical (RXT) and maximum (RXM) formulations of this coating. In the second cycle of testing the Rain-X–

MP-55 peak loads increased significantly and were no longer separated from some of the other coatings tested.

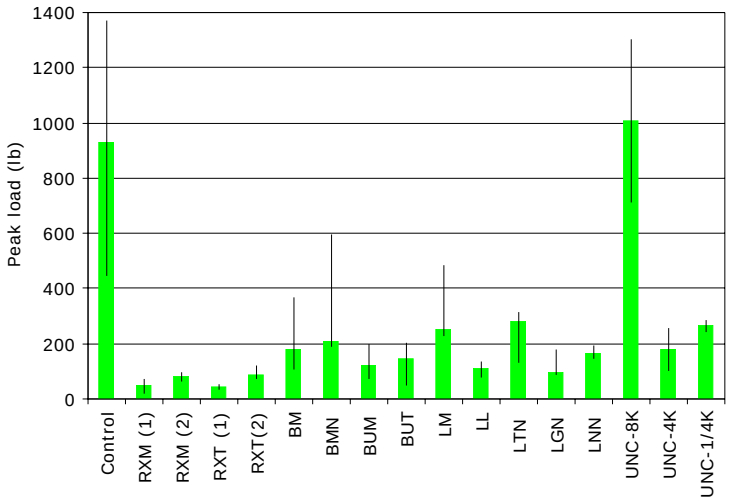


a. All controls and coatings tested in phase 1.

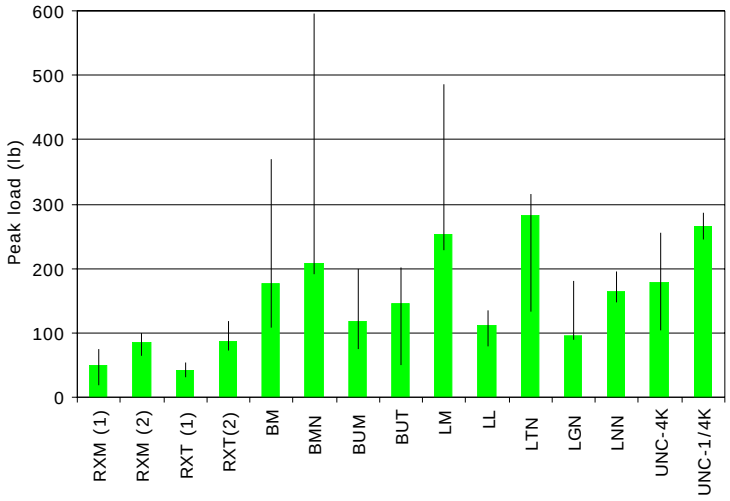


b. Expanded scale, not including controls and UNC-8K coating.

Figure 26. Bar charts of peak loads with bar height representing the median peak load of the group, and the error bar indicating the corresponding minimum and maximum.

## Work-Power and Stick-Slip Analyses of Load-Time Response

Mean values of work and power are given for each coating by strain rate in Figures 27 and 28, respectively. At the low strain rate the work required (Fig. 27) is highest for the controls and the UNC-8K coating while the cycle 1 RXM and RXT coatings develop the least work. The work required at high strain rate for the Braycote and lithium grease coatings increase significantly, while both cycles of the RXM and RXT coatings show outstanding performance. The power comparisons given in Figure 28 are much the same as those of work, indicating that variable load application times are not significantly affecting the results. Behind RXM–RXT, the BUM and BUT coatings are next most effective at both strain rates, as measured by both power and work.

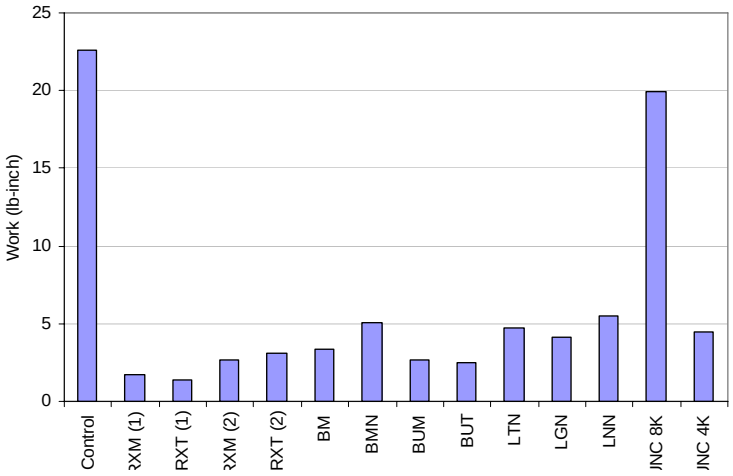


a. Low strain rate.

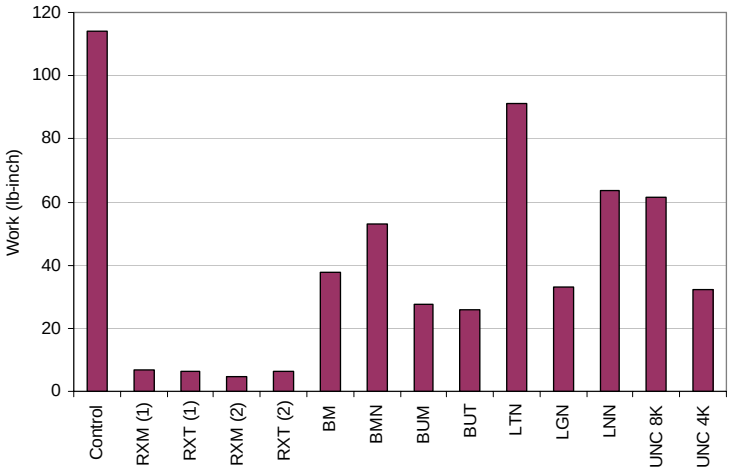


b. High strain rate.

Figure 27. Work expended for each phase 1 coating.

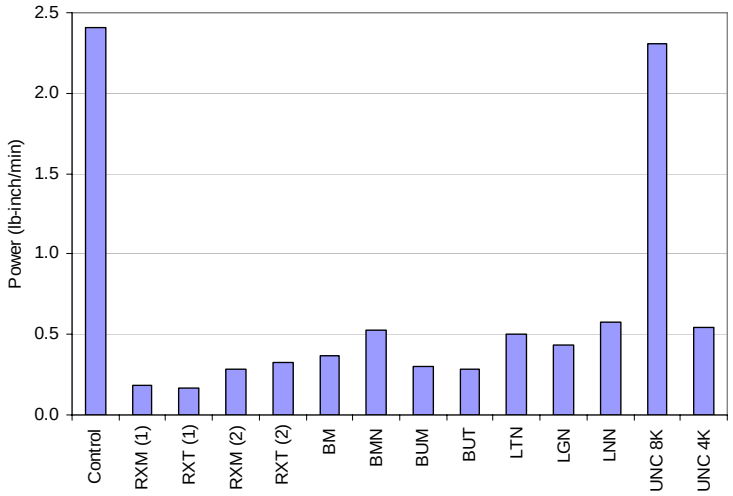


a. Low strain rate.

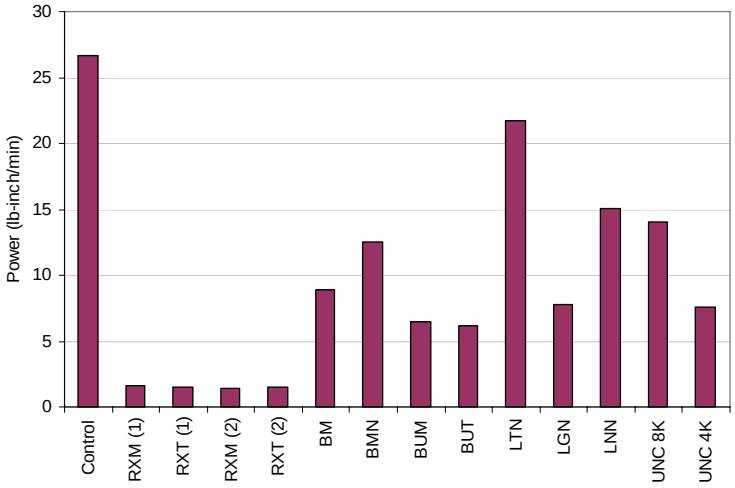


b. High strain rate.

Figure 28. Power expended for each phase 1 coating.

Results of short-term "stick–slip" load variability calculations of several RXM tests are shown in Figure 29, presenting sequential standard deviations from the mean over 12-second time segments, with data subdivided by strain rate and test cycle. At low strain rate there is no trend in the standard deviations with time through the tests, but the cycle 2 values are greater than those of cycle 1. At high strain rate, there may be a slight decrease with time in the standard deviations, and, here, the cycle 2 values are only slightly greater than those of cycle 1. Without important temporal trends, each graph of Figure 29 can be represented by a single value, the average standard deviation over all time intervals of a test and all coupons of a group.

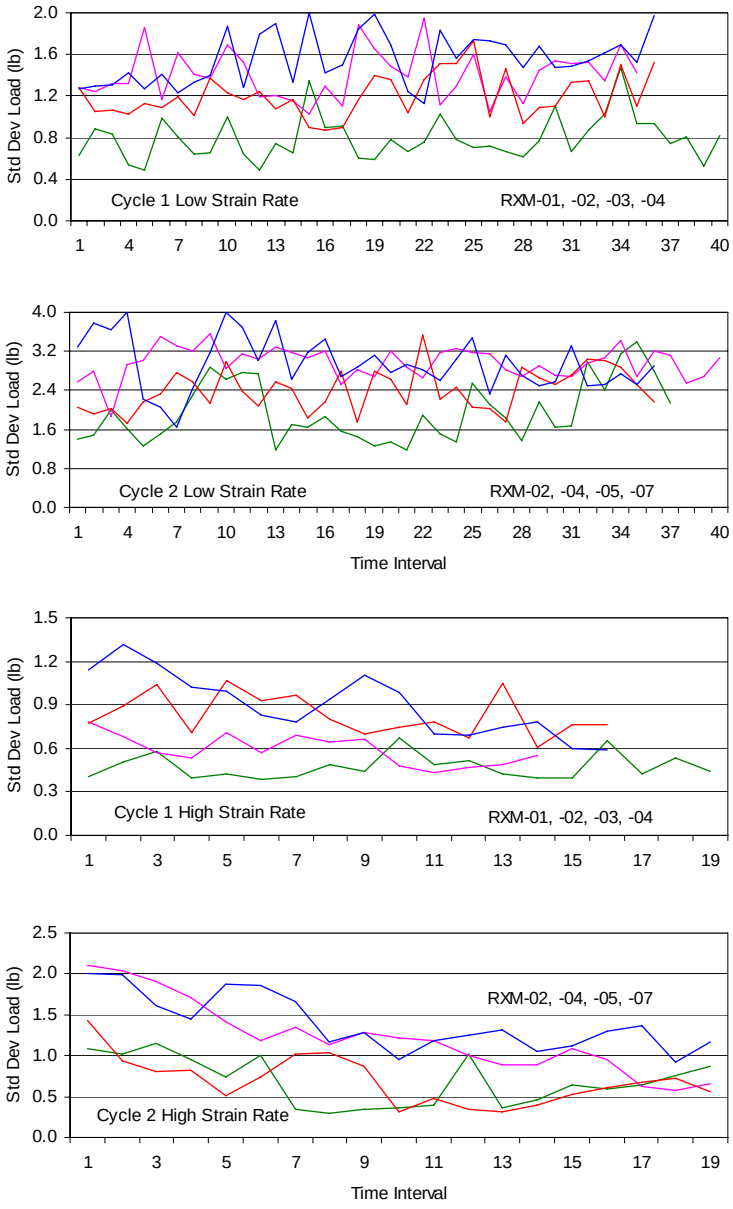


**Figure 29. Time sequence of standard deviations from the mean load over 12 sec intervals for several RXM samples: (top) low strain rate, cycle 1; (second) low strain rate, cycle 2; (third) high strain rate, cycle 1; (bottom) high strain rate, cycle 2.**

These averages are presented for all coatings and cycles of phase 1 testing in Figure 30 for both strain rates. Very large average standard deviations of the load are associated with the low strain rate saw-tooth loads of both the controls and the UNC-8K coating. The small decrease in these deviations at the high strain rate was probably a result of accumulated damage to the ice. The average standard deviations are also quite high for both strain rates of the UNC-4K coating, but all other coatings have much

smaller values. It is clear from the expanded scale plot in Figure 30 that the Rain-X coatings displayed larger standard deviations at low versus high strain and for low strain in cycle 2 versus cycle 1, consistent with the more detailed data of Figure 29. Though Braycote and lithium grease loads generally varied with strain rate, the standard deviations, with the exception of LTN, were not strain rate sensitive.

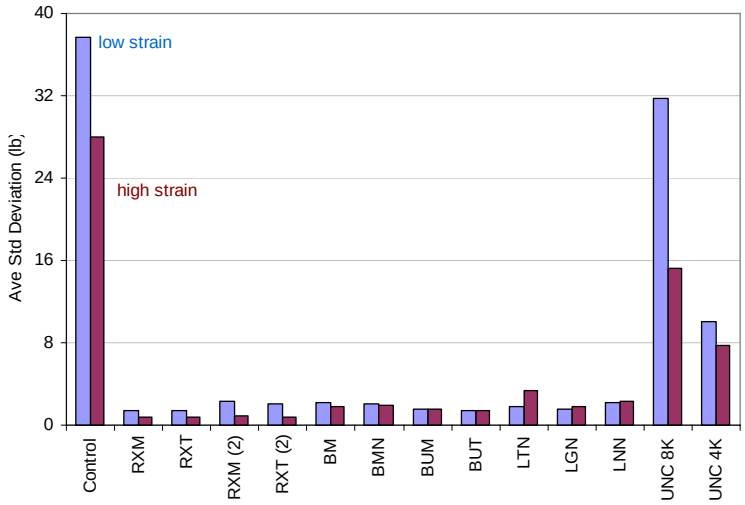


a. Controls and all coatings.

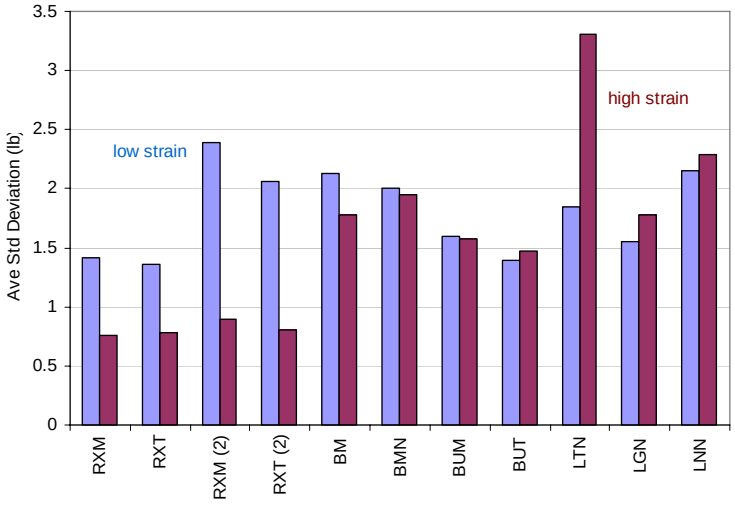


b. Expanded scale with controls and UNC samples deleted.

Figure 30. Average standard deviation (lb) from the mean load over successive 12-second intervals of each test, averaged again for each phase 1 coating, and given by strain rate.

## Phase 1 Conclusions

The phase 1 tests showed that Rain-X mixed with MP-55 was an outstanding coating to reduce ice adhesion to Koropon coated aluminum at cryogenic temperatures. Significant amounts of coating retained on the ice surface indicated failure in the RXM coating and the potential for loss of effectiveness with repeated cycles of ice formation and release. As the RXM coating durability was not fully established by the phase 1 results, uncertainty remained concerning its use in critical areas. The overall consistency and performance of the BUM coating indicated superiority of UF-8TA over MP-55 when mixed with Braycote. As UF-8TA was not mixed with Rain-X, potential performance and consistency improvements to the RXM coating remain to be quantified.

# 7 Phase 2 Test Results

The purpose of the phase 2 investigations was to evaluate potential modifications to the RXM coating that would maintain effectiveness and enhance durability. Variations of the Rain-X–MP-55 maximum mix, with DF 1040 substituted for some of the Rain-X, were applied to coupons having a primer coat of DC 1200. Five coupons of each of 3 mixes, 10, 5 and 0% DF 1040, were tested through three cycles, and selected coupons of each mix with high performance were tested in a fourth cycle.

## 10% DF 1040

The most typical load–time responses of the 10% mix, as determined by near average total work and peak load, are given in Figure 31 for each of the three cycles. The mean and standard deviation of total work and peak load for these series are given in Table 7, along with the corresponding ranges. Total work and peak load were both more consistent in the first cycle than in the later cycles. Mean total work was constant in the first two cycles before decreasing in the third cycle, while mean peak load increased from the first to the second cycle, and then decreased to the first cycle value in cycle 3. Load generally decreased with increased strain rate in all three cycles. There was post-test evidence of some ice fracture initiated at the planar interface with the coupon, and coating material was retained on the ice surface in all three cycles.

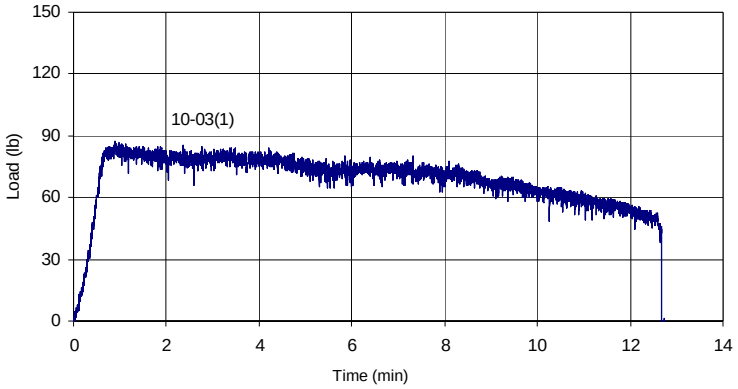


a. Coupon 03, cycle 1.

Figure 31. Most typical load–time trace in each of three cycles for 10% mixture of DF 1040 with Rain-X and MP-55 maximum. "Typical" is the coupon with the closest peak load and total work to the averages for the group.

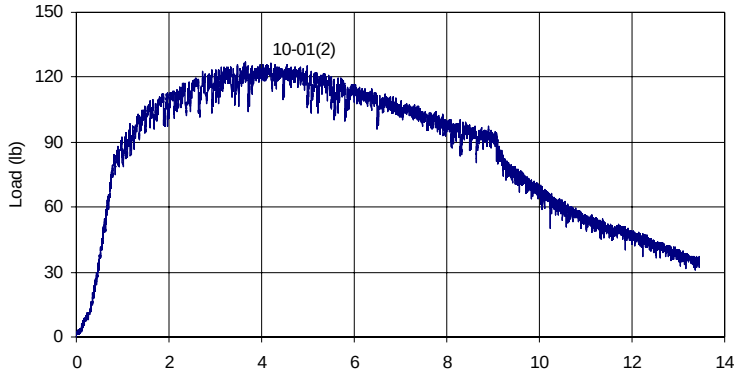


b. Coupon 01, cycle 2.

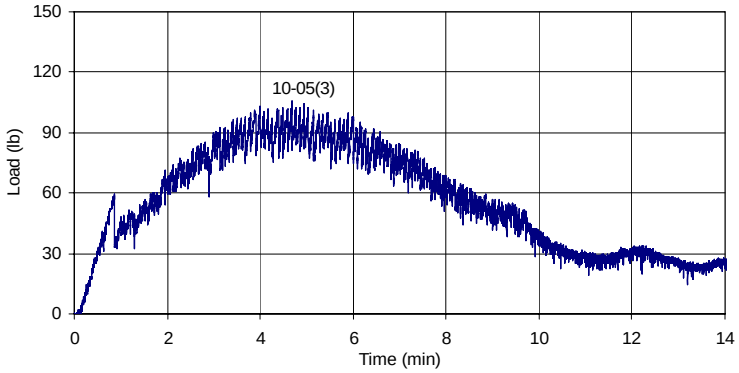


c. Coupon 05, cycle 3.

Figure 31 (cont'd). Most typical load–time trace in each of three cycles for 10% mixture of DF 1040 with Rain-X and MP-55 maximum. "Typical" is the coupon with the closest peak load and total work to the averages for the group.

Table 7. Comparison of Phase 2 durability results.

| Formulation (% DF1040) | Cycle | Total work mean ±s.d. (lb-in.) | Work range (lb-in.) | Peak load mean ±s.d. (lb) | Peak load range (lb) |
|---|---|---|---|---|---|
| 10 | 1 | 32 ± 6 | 24–41 | 96 ± 12 | 85–119 |
| | 2 | 33 ± 16 | 17–64 | 152 ± 36 | 92–190 |
| | 3 | 19 ± 16 | 4-49 | 92 ± 43 | 22–135 |
| 5 | 1 | 42 ± 10 | 30–56 | 124 ± 32 | 71–164 |
| | 2 | 35 ± 5 | 29–41 | 128 ± 25 | 102–174 |
| | 3 | 23 ± 5 | 16–29 | 80 ± 17 | 56–103 |
| 0 | 1 | 41 ± 7 | 33–50 | 139 ± 20 | 102–160 |
| | 2 | 23 ± 11 | 6–37 | 88 ± 33 | 34–123 |
| | 3 | 23 ± 5 | 7–28 | 58 ± 23 | 31–87 |

## 5% DF 1040

The most typical load–time responses of the 5% mix are given in Figure 32 for each of the three cycles. The mean and standard deviation of total work and peak load for these series are given in Table 7, along with the corresponding ranges. Mean total work decreased with cycling, and mean peak load decreased in cycle 3 relative to cycles 1 and 2. Variability in total work and peak load also decreased with cycling of the coupons. During individual tests in all cycles, the load generally decreased with the increase in strain rate. Post-test analysis following each cycle revealed smooth planar ice surfaces at the interface with the coupon, some fracturing of the ice, and coating material retained on the ice.

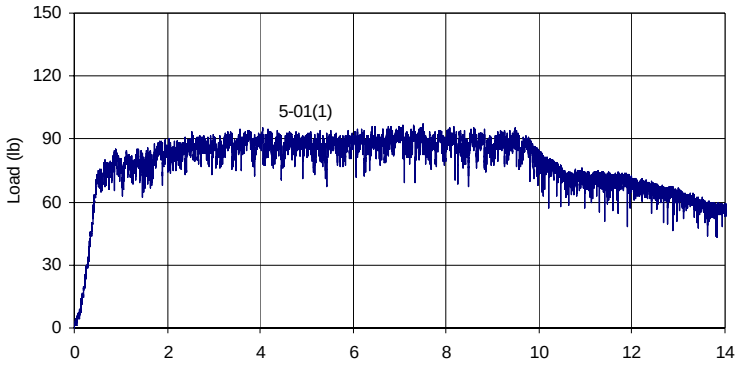


a. Coupon 01, cycle 1.

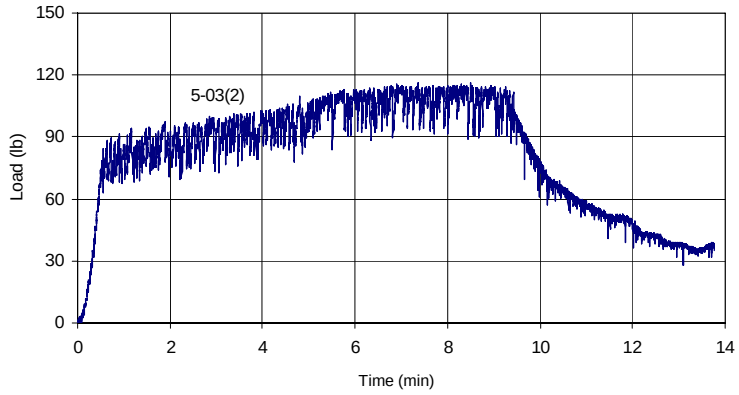


b. Coupon 03, cycle 2.

Figure 32. Most typical load–time trace in each of 3 cycles for 5% mixture of DF 1040 with Rain-X and MP-55 maximum.

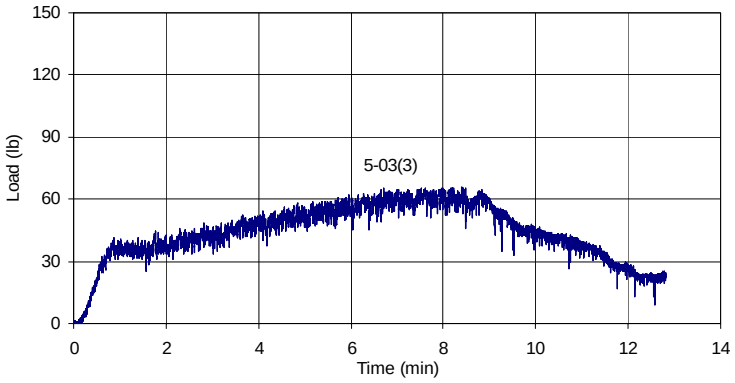


c. Coupon 03, cycle 3.

Figure 32 (cont'd). Most typical load–time trace in each of 3 cycles for 5% mixture of DF 1040 with Rain-X and MP-55 maximum.

## 0% DF 1040

The most typical load–time responses of the 0% mix are given in Figure 33 for each of the three cycles. The mean and standard deviation of total work and peak load for these series are given in Table 7, along with the corresponding ranges. Mean total work and peak load decreased in successive cycles, while variability in these parameters was unchanged between the first and third cycles. During individual tests in all cycles, the load generally decreased with the increase in strain rate. Post-test analysis following each cycle again revealed smooth planar ice surfaces at the interface with the coupon, some fracturing of the ice, and coating material retained on the ice.

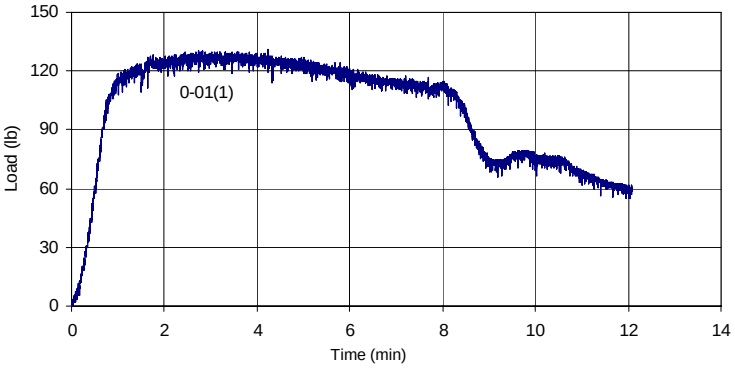


a. Coupon 01, cycle 1.

Figure 33. Most typical load–time trace in each of three cycles for 0% mixture of DF 1040 with Rain-X and MP-55 maximum.

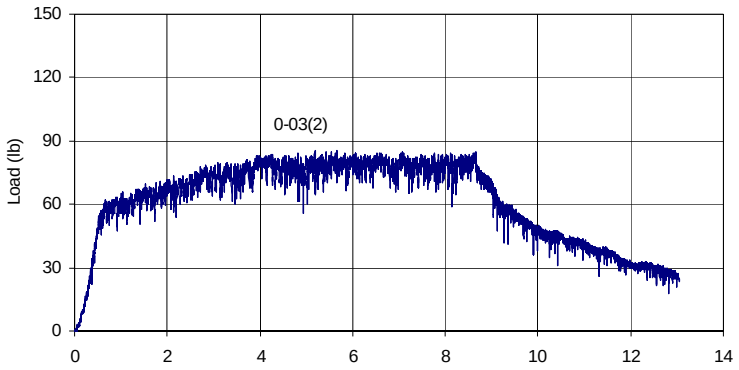


b. Coupon 03, cycle 2.

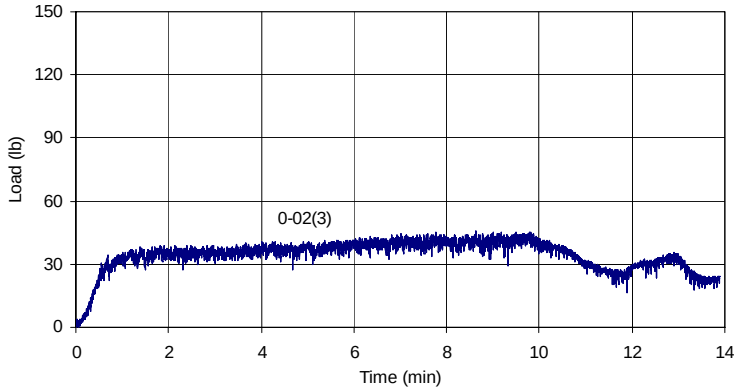


c. Coupon 02, cycle 3.

Figure 33 (cont'd). Most typical load–time trace in each of three cycles for 0% mixture of DF 1040 with Rain-X and MP-55 maximum.

## Preliminary Comparisons

The performance of the 10% mix generally improved through the cycles, but variability in total work and peak load were greatest in cycle 3. The 5% mix achieved minimum total work and peak load in cycle 3, comparable to those of the 10% mix, but with much less variability. The 0% mix also improved through cycle 3, with total work and peak load performance in that cycle comparable to or slightly better than the 5% mix. The three best coupons from each mix were tested in a fourth cycle, and total work and peak load for each of these coupons are given by test cycle in Figures 34 and 35, respectively. Both parameters generally decreased through the first three test cycles for these coupons, consistent with the Table 7 data for the full sample groups. However, total work in cycle 4 was comparable to that in

cycle 3, while peak loads were comparable to or greater than those of cycle 3, indicating that performance does not improve indefinitely with cycling.

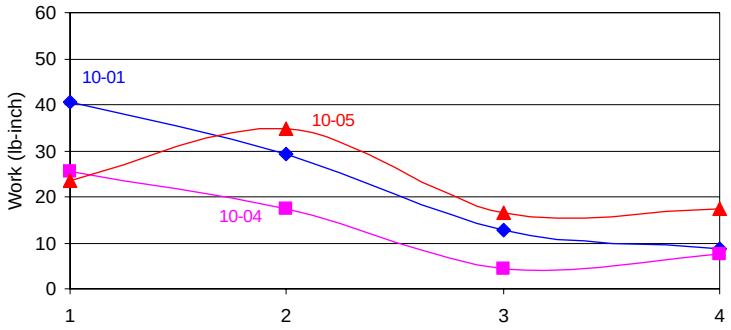


a. 10% DF 1040.

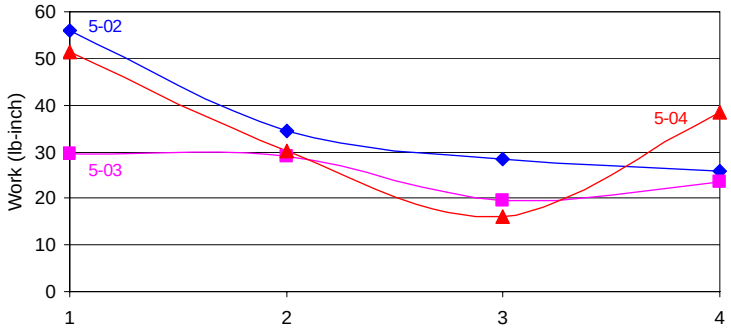


b. 5% DF 1040.

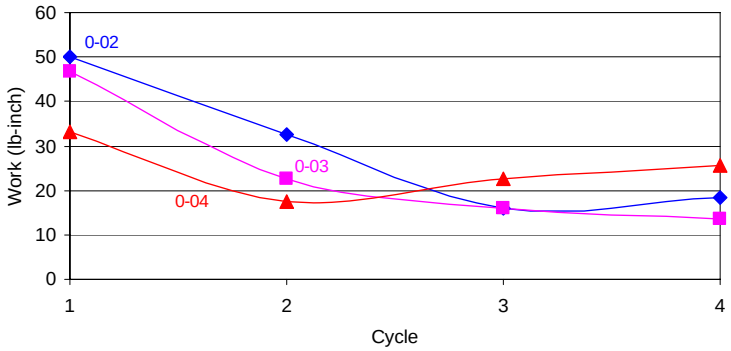


c. 0% DF 1040.

Figure 34. Total work for individual coupons tested over four cycles in phase 2.

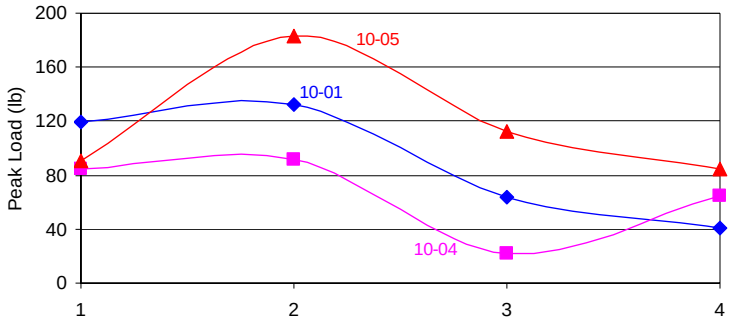


a. 10% DF 1040.

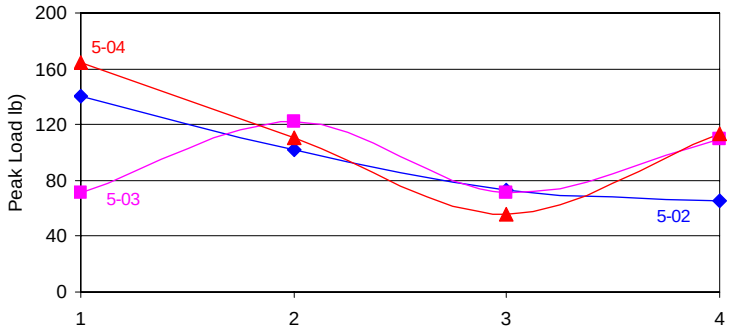


b. 5% DF 1040.

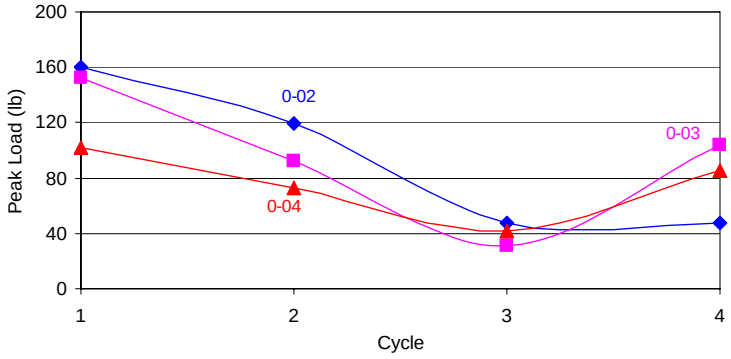


c. 0% DF 1040.

Figure 35. Peak load for individual coupons tested over four cycles in phase 2.

Each of the phase 2 coatings was visually similar through the three cycles of double lap shear testing. Figure 36 documents changes in coating appearance in response to multiple test cycles. Figure 36a depicts untested (10-7, 0-7) phase 2 coupons, coupons after one test cycle (0-4, 0-5), and

coupons after two test cycles (10-4, 10-5). Figure 36b compares phase 2 coupons after four test cycles (0-2, 0-3, 0-4, 5-2, 10-5) with phase 1 coupons after three cycles (RXM-2, RXM-8). The progressive loss of coating material from the coupons is evident through the test cycles, and yet coating performance does not degrade. The residual coating that can be seen visually is least for the RXM coupons after three cycles, and yet their total work performance (Table 6, Fig. 24) is better than all phase 2 coatings.

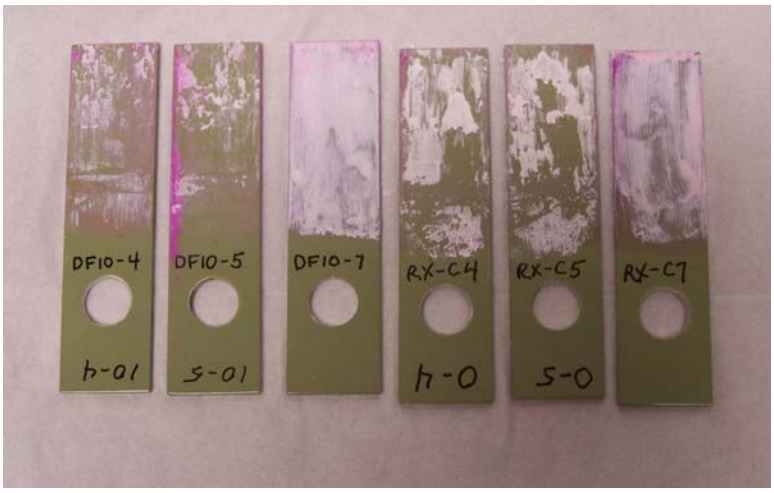


a. After two cycles (10-04, 10-05), after one cycle (0-04, 0-05), and untested (10-07, 0-07) phase 2 coupons.

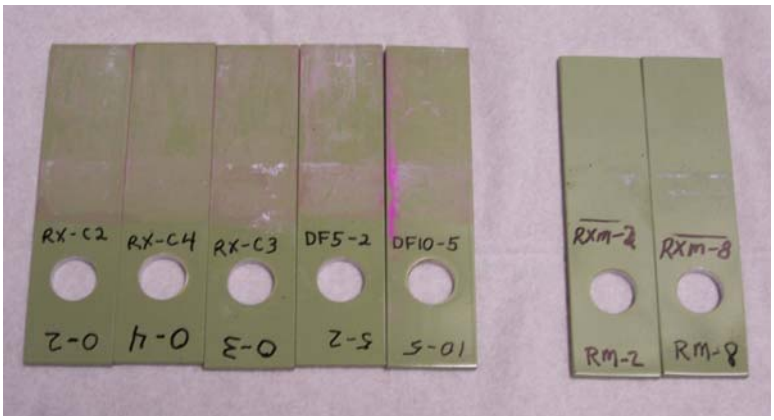


b. After four cycles (0-02, 0-03, 0-04, 5-02, 10-05) for phase 2 coupons, and after three cycles (RXM-02, RXM-08) for phase 1 coupons.

Figure 36. Visual changes in coating appearance in response to multiple cycles of double lap shear testing.

## Analysis of Load–Time Response

Figure 37 gives median, minimum, and maximum peak loads for all phase 2 coatings and cycles, along with phase 2 controls and corresponding phase 1 cycle 3 RXM data. The Kruskal-Wallis test indicates no significant statistical difference among the peak load performances of any of the phase 2 variations. Average work and power were again computed for each test as a pair of values, one for the initial low strain rate and a second for the high strain rate that was applied later. Mean values of work and power are given for each coating, by strain rate, in Figures 38 and 39, respectively. At both strain rates, the average work (Fig. 38) was again highest with the controls and generally decreased with cycling for all three coatings investigated. At low strain the best performing phase 2 test groups are comparable to the RXM–cycle 3 results of phase 1 that represent the best coupons from that group. However, none of the phase 2 groups achieved comparable work to RXM (3) at high strain. The trends and comparisons of power given in Figure 39 are much the same as those of work at both strain rates. The best phase 2 coating and cycle generated more average work and power than the best phase 1 coating, RXM (3).

The short-term variability of the load or "stick–slip" behavior of phase 2 tests was again characterized by the standard deviation from the mean load over 12 second time-intervals averaged over all time intervals of a given strain rate/test, and all tests of a group. These averages are presented in Figure 40 for both strain rates and all coatings and cycles of phase 2 testing. Large average standard deviations of the load in the same range as for phase 1 are again associated with the controls, but in these tests the larger variability occurred at high instead of low strain rate. The average standard deviations for all coated samples were much smaller, as before. The expanded scale plot in Figure 40 shows that the phase 2 Rain-X coatings again displayed larger average standard deviations at low versus high strain rate. Also, the phase 2 average standard deviations are very consistent in cycles 3 and 4, and comparable to RXM cycle 3 of phase 1.

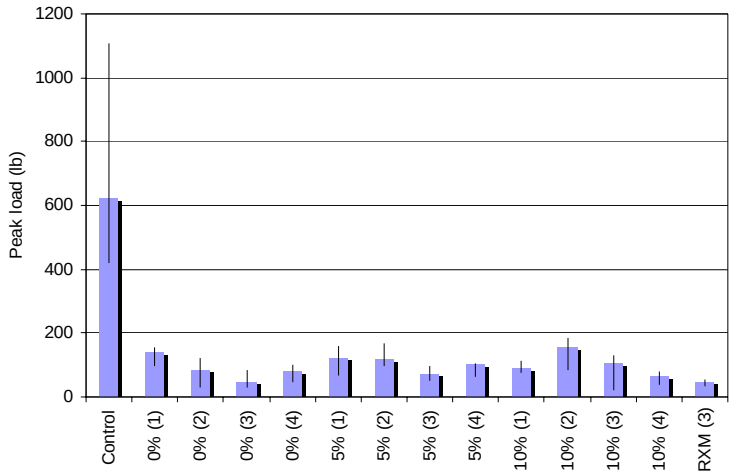


a. All controls and coatings tested in phase 2 plus RXM cycle 3 results for comparison.

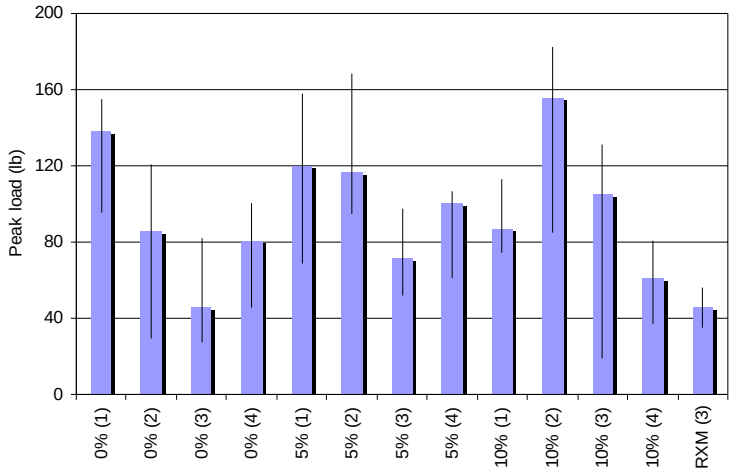


b. Expanded scale, not including controls.

Figure 37. Bar charts of peak loads with bar height representing the median peak load of the group, and the error bar indicating the corresponding minimum and maximum.

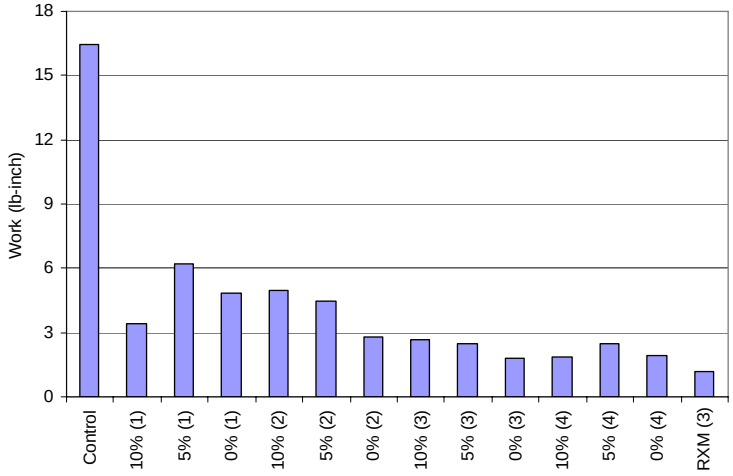


a. Low strain rate.

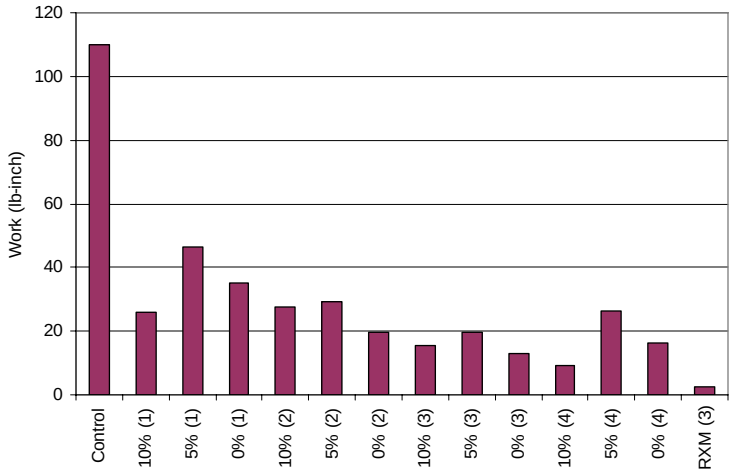


b. High strain rate.

Figure 38. Average work expended for each phase 2 coating.

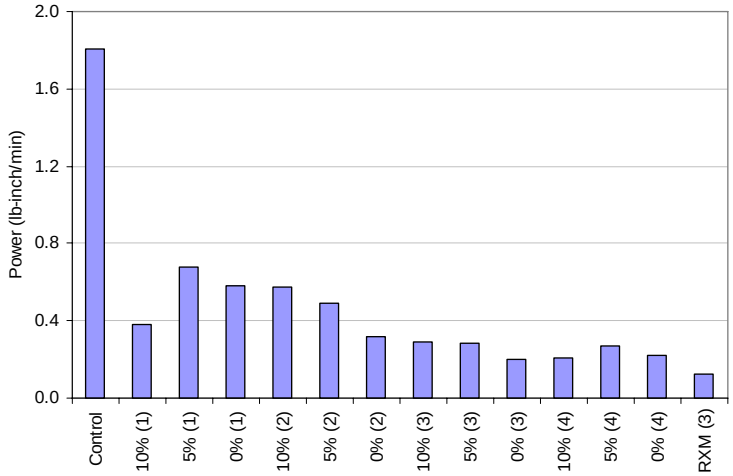


a. Low strain rate.

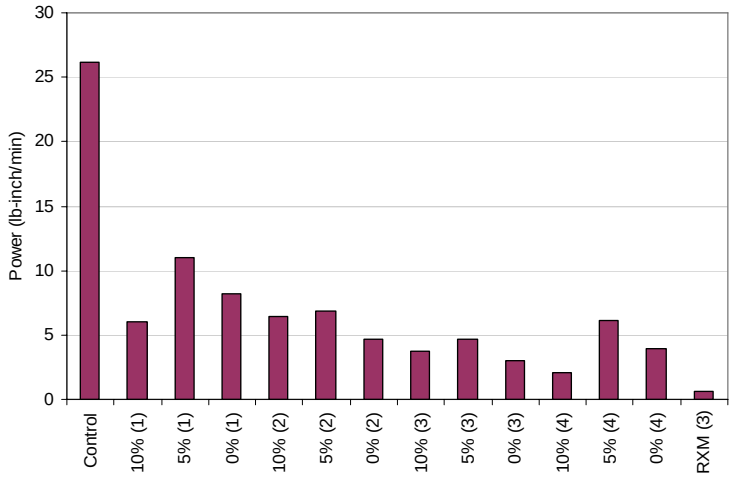


b. High strain rate.

Figure 39. Average power expended for each phase 2 coating.

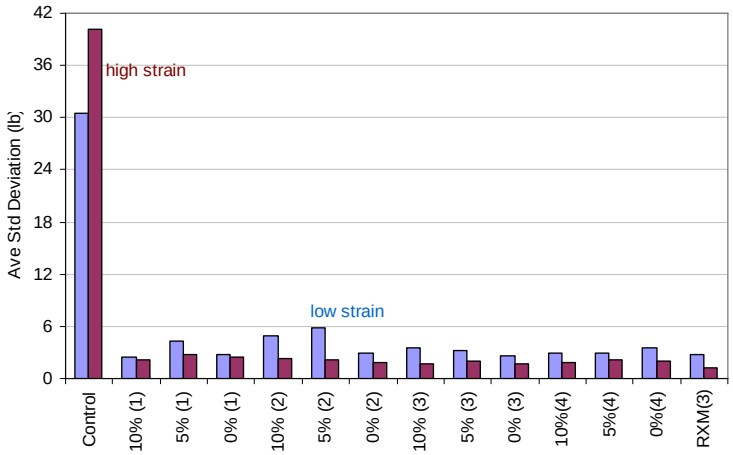


a. Controls and all coatings.

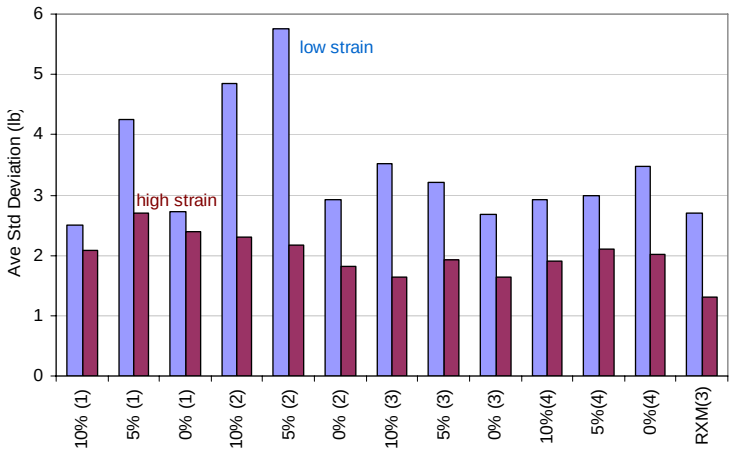


b. Expanded scale with controls deleted.

Figure 40. Average standard deviation (lb) from the mean load over successive 12-second intervals of each test, averaged again for each phase 2 coating, and given by strain rate.

## Phase 2 Conclusions

The addition of DF 1040 in phase 2 to the original Rain-X–MP-55 maximum mixture did not improve the ice adhesion performance at cryogenic temperature or coating durability. Like the original, coating material is lost in each test cycle with all DF 1040 mixes, but effectiveness of the remaining coating improved through three cycles and then remained constant in cycle 4. Comparison of the 0% phase 2 and RXM–RXT phase 1 results indicate that the DC 1200 primer slightly degraded the performance of the

original coating. However, at this stage of the testing program, the original RXM–RXT coating still has unresolved durability, workability, and application questions.

# 8 Phase 3 Test Results

The phase 3 investigations consider variations in mixing procedures of the Rain-X–MP-55 maximum mixture, effects of wiping off the coating following application and curing, and effects of subjecting the coating to a water stream. Ten coupons of each of three mixes—RM, RP, and RD—were tested through three cycles. Five coupons of each group had the coating applied and left undisturbed ('a' sample groups), while five other coupons of each group were coated and wiped off after a short curing time ('b' sample groups). In addition, three coupons of RP type, designated RW, were not wiped but subjected to a water stream after curing.

## Cycle 1: All Mixes, Treatments

The most typical load–time responses of the RM and RP mixes in cycle 1, as determined by near average total work and peak load, are given in Figure 41. The loads developed by the wiped coupons in both of these groups were substantially higher throughout the tests than those of the coupons that were not wiped. Similarly, Figure 42 gives the most typical load–time responses of the RD and RW mixes in cycle 1. The wiped RD samples developed much higher loads than all the other samples in cycle 1, requiring a larger load scale in Figure 42. The implication of these findings is that the coating must remain on the surface for a much longer time prior to any wiping-off operation. The 1.5-hour curing prior to wiping the RM(b) and RP(b) samples was much better than the 0.5-hour time allotted to the RD(b) samples, but still not adequate for optimal performance. The mean ± standard deviation, median, maximum, and minimum of total work and peak load are summarized for cycle 1 in Table 8. The RM(a) group had an anomalous sample, RM-02, which exhibited much higher adhesion than all other samples of the same group. With this sample discounted, the RM(a) and RP(a) groups performed similarly in cycle 1 with respect to peak load and total work. The RD(a) and RW(a) groups also performed similarly. Load generally decreased with increased strain rate in the cycle 1 tests. There was post-test evidence of some ice fracture initiated at the planar interface with the coupon, especially in the wiped (b) sample groups. For all sample groups, coating material was retained on the ice surface following the tests.

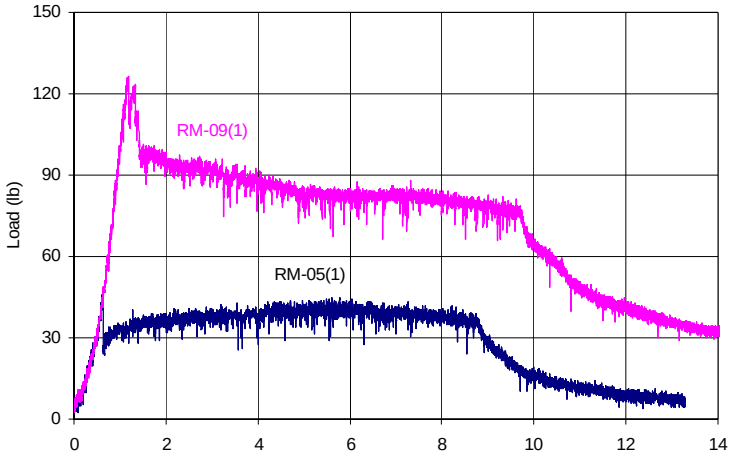


a. RM coupons 05 (not wiped) and 09 (wiped).

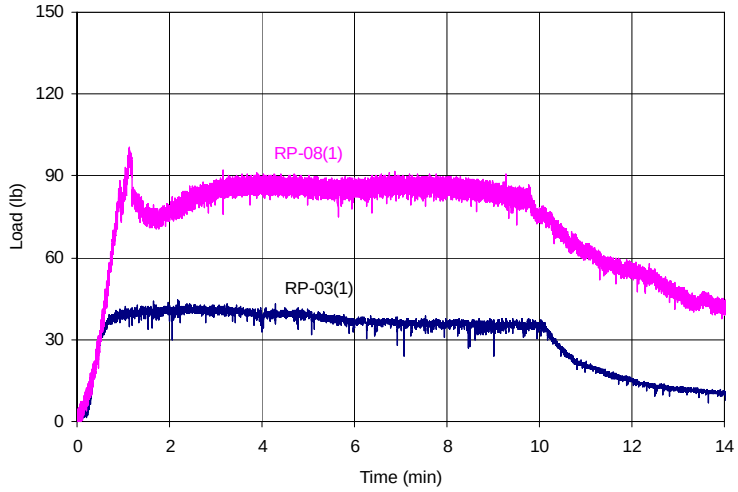


b. RP coupons 03 (not wiped) and 08 (wiped).

Figure 41. Most typical load–time traces for Rain-X and MP-55 maximum mixtures in cycle 1 of phase 3.

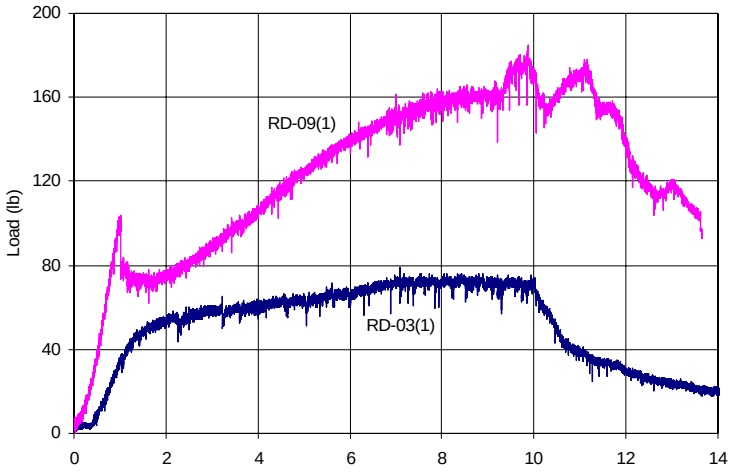


a. RD coupons 03 (not wiped) and 09 (wiped).

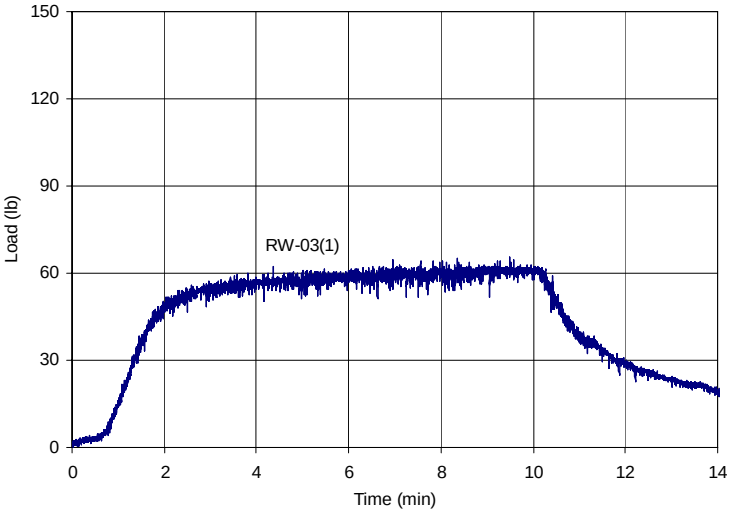


b. RW coupon 03 (not wiped).

Figure 42. Most typical load–time traces for Rain-X and MP-55 maximum mixtures in cycle 1 of phase 3. Note the increased load scale of the RD cycle 1 plot relative to RW, RM, and RP.

Table 8. Phase 3 peak load and total work summaries: Cycle 1.

| | Peak Load (lb) | | | |
|---|---|---|---|---|
| Group | Mean ± Std Dev | Median | Maximum | Minimum |
| Controls: all cycles (18) | 559 ± 117 | 541 | 865 | 412 |
| RM (a) | 61 ± 26 | 49 | 110 | 37 |
| RM (a) minus sample 2 | 49 ± 10 | 47 | 65 | 37 |
| RM (b) | 125 ± 25 | 128 | 152 | 94 |
| RP (a) | 48 ± 9 | 49 | 60 | 33 |
| RP (b) | 97 ± 20 | 100 | 129 | 68 |
| RD (a) | 67 ± 13 | 71 | 82 | 51 |
| RD (b) | 201 ± 53 | 217 | 259 | 106 |
| RW (a) | 69 ± 18 | 67 | 93 | 48 |
| | Total Work (lb-inch) | | | |
| Group | Mean ± Std Dev | Median | Maximum | Minimum |
| Controls: all cycles (18) | 137 ± 22 | 134 | 179 | 97 |
| RM (a) | 11.4 ± 7.7 | 8.1 | 26.7 | 6.7 |
| RM (a) minus sample 2 | 7.5 ± 0.7 | 7.5 | 8.4 | 6.7 |
| RM (b) | 21.7 ± 5.5 | 23.8 | 28.9 | 13.8 |
| RP (a) | 9.7 ± 1.8 | 10.1 | 11.5 | 6.4 |
| RP (b) | 27.4 ± 5.6 | 29.5 | 34.1 | 20.5 |
| RD (a) | 16.6 ± 4.8 | 17.1 | 24.1 | 10.3 |
| RD (b) | 61.4 ± 16.5 | 70.8 | 74.6 | 30.8 |
| RW (a) | 17.2 ± 2.9 | 16.5 | 21.0 | 14.1 |

An important observation from late September 2005 was that when the Koropon-coated aluminum coupons were dipped into the very brightly colored DC 1200 primer, about 10% of the specimens exhibited sizeable areas of irregularity in the Koropon. This irregularity indicated poorly mixed Koropon where a catalyst or hardener may not have been uniformly dispersed, a result that is not unusual in hand-mixing operations. As DC 1200 was not used in phase 3, such non-uniformities in the Koropon coating could not be detected. A possible method to detect these imperfections may be with UV light, and this experiment should be conducted. Surface non-uniformity may cause outliers in the double lap shear results, like sample RM-02; however, other factors may also contribute to these anomalous results.

## Cycle 2: All Mixes, Treatments

The most typical load–time responses of the RM, RP, RD(a), and RW(a) mixes in cycle 2, as determined by near average total work and peak load, are given in Figure 43. The ice adhesion developed by the wiped coupons in both of the RM and RP groups were substantially higher throughout the tests than those of the coupons that were not wiped. The non-wiped RD samples performed almost as well as the non-wiped RP samples, and better than the non-wiped RW samples in cycle 2.

Table 9. Phase 3 peak load and total work summaries: Cycle 2.

| | Peak Load (lb) | | | |
|---|---|---|---|---|
| Group | Mean ± Std Dev | Median | Maximum | Minimum |
| RM (a) | 25 ± 14 | 19 | 51 | 12 |
| RM (a) minus sample 2 | 19 ± 5 | 19 | 26 | 12 |
| RM (b) | 68 ± 17 | 63 | 95 | 46 |
| RP (a) | 28 ± 6 | 30 | 36 | 17 |
| RP (b) | 81 ± 19 | 90 | 102 | 56 |
| RD (a) | 33 ± 14 | 28 | 52 | 18 |
| RD (b) only 2 samples | 171 | -- | 246 | 95 |
| RW (a) | 54 ± 7 | 52 | 64 | 46 |
| | Total Work (lb-inch) | | | |
| Group | Mean ± Std Dev | Median | Maximum | Minimum |
| RM (a) | 6.6 ± 5.9 | 3.7 | 16.7 | 2.2 |
| RM (a) minus sample 2 | 3.2 ± 1.1 | 2.7 | 4.8 | 2.2 |
| RM (b) | 11.2 ± 1.7 | 11.0 | 14.2 | 9.2 |
| RP (a) | 5.9 ± 1.9 | 6.2 | 8.4 | 2.6 |
| RP (b) | 23.7 ± 6.6 | 27.5 | 31.1 | 15.7 |
| RD (a) | 5.7 ± 2.4 | 6.5 | 9.2 | 2.2 |
| RD (b) only 2 samples | 53.2 | -- | 76.5 | 29.9 |
| RW (a) | 13.0 ± 1.2 | 12.5 | 14.6 | 11.8 |

The mean ± standard deviation, median, maximum, and minimum of total work and peak load are summarized for cycle 2 testing in Table 9. The RM(a) group again had anomalous sample RM-02, which exhibited much higher adhesion than all other samples of the group. Discounting this sample, the RM(a) group performed optimally with respect to peak load and total work in cycle 2. Again, load generally decreased with increased

strain rate in the cycle 2 tests. There was post-test evidence of some ice fracture initiated at the planar interface with the coupon, especially in the wiped (b) sample groups. For all sample groups, coating material was again retained on the ice surface following the tests.

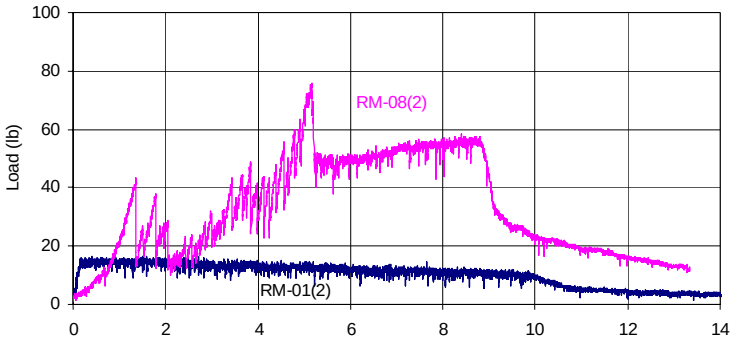


a. RM coupons 01 (not wiped) and 08 (wiped).

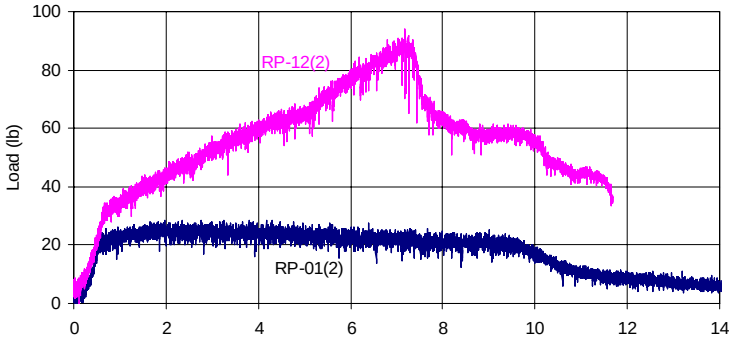


b. RP coupons 01 (not wiped) and 12 (wiped).

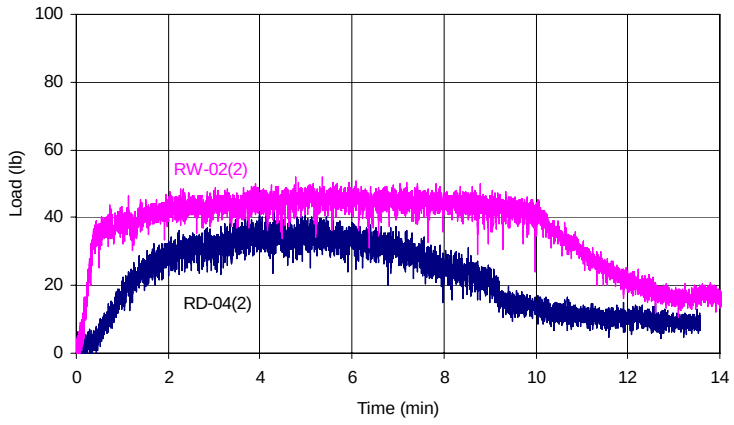


c. RD coupon 04 (not wiped) and RW coupon 02 (not wiped).

Figure 43. Most typical load–time traces for Rain-X and MP-55 maximum mixtures in cycle 2 of phase 3. Note the decreased load scale relative to the cycle 1 plots.

## Cycle 3: All Mixes, Treatments

The most typical load–time responses of the RM, RP, RD(a), and RW(a) mixes in cycle 3, as determined by near average total work and peak load, are given in Figure 44. Again, load generally decreased with increased strain rate in these tests. The ice adhesion developed by the non-wiped coupons of both the RM and RP groups were extremely low, but the adhesion to wiped samples of both these groups was substantially higher. The non-wiped RD samples again outperformed the non-wiped RW samples in cycle 3. The mean ± standard deviation, median, maximum, and minimum of total work and peak load are summarized for all cycle 3 mixes and treatments in Table 10. RM-02 again appears as an anomalous sample with much higher adhesion than all other samples of the group. With this sample discounted, the RM(a) and RP(a) groups both displayed optimal peak load and total work performance in cycle 3. An anomalous high adhesion sample appeared for the first time in the RD(a) group in cycle 3. However, the performance of all mixes and treatments generally improved through the cycles. There was post-test evidence of some ice fracture initiated at the planar interface with the coupon, especially in the wiped (b) sample groups. For all sample groups, coating material was again retained on the ice surface following the tests, though less than in earlier cycles.

## Visual Comparisons

Each of the phase 3 coating mixes and treatments were visually similar through the three cycles of double lap shear testing. Figure 45 documents visual changes in the appearance of the RM coating after each test cycle. Figure 45a depicts both wiped and non-wiped subgroups after one test cycle. Whitish coating material can be seen on the coupon surfaces of both groups. Figure 45b depicts the same coupons having less visible coating remaining after two test cycles, and Figure 45c shows these coupons after three test cycles. The progressive loss of coating material from the coupons is evident through the test cycles, even for the wiped coupons. As in phase 2, this loss of coating material was accompanied by improved performance of the remaining coating.

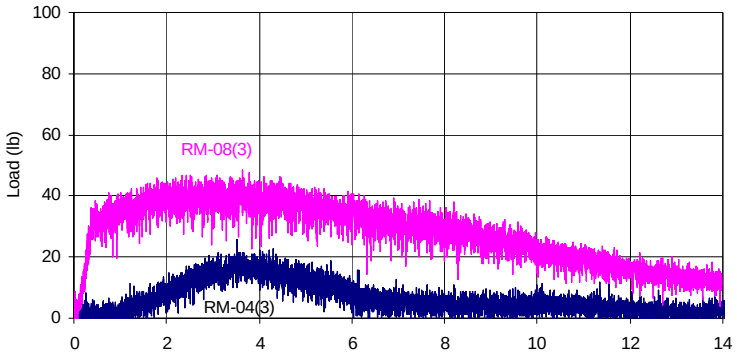


a. RM coupons 04 (not wiped) and 08 (wiped).

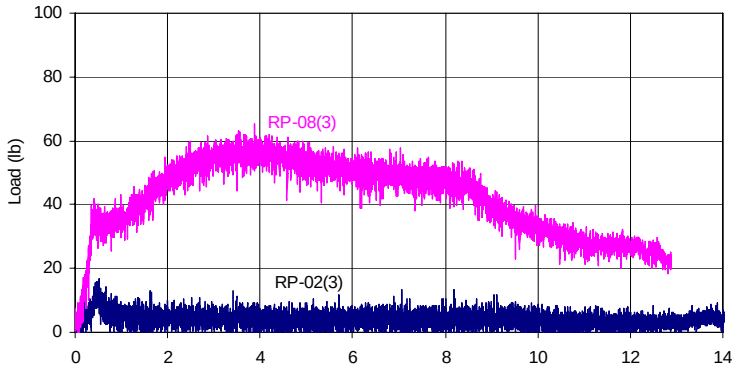


b. RP coupons 02 (not wiped) and 08 (wiped).

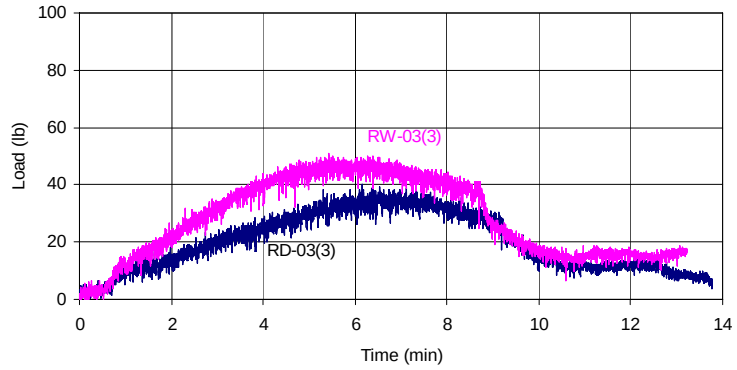


c. RD coupon 03 (not wiped) and RW coupon 03 (not wiped).

Figure 44. Most typical load–time traces for Rain-X and MP-55 maximum mixtures in cycle 3 of phase 3. Note the decreased load scale relative to the cycle 1 plots.

Table 10. Phase 3 peak load and total work summaries: Cycle 3

| | Peak Load (lb) | | | |
|---|---|---|---|---|
| Group | Mean ± Std Dev | Median | Maximum | Minimum |
| RM (a) | 28 ± 20 | 19 | 66 | 10 |
| RM (a) minus sample 2 | 19 ± 9 | 17 | 32 | 10 |
| RM (b) | 48 ± 14 | 44 | 75 | 34 |
| RP (a) | 15 ± 5 | 13 | 25 | 11 |
| RP (b) | 65 ± 22 | 60 | 105 | 39 |
| RD (a) | 43 ± 26 | 41 | 91 | 19 |
| RD (a) minus sample 2 | 31 ± 11 | 32 | 42 | 19 |
| RD (b) only 2 samples | 131 | -- | 172 | 89 |
| RW (a) | 48 ± 2 | 46 | 51 | 46 |
| | Total Work (lb-inch) | | | |
| Group | Mean ± Std Dev | Median | Maximum | Minimum |
| RM (a) | 6.0 ± 8.5 | 1.8 | 22.9 | 0.3 |
| RM (a) minus sample 2 | 1.8 ± 1.2 | 1.7 | 3.2 | 0.3 |
| RM (b) | 9.6 ± 1.6 | 9.6 | 12.2 | 7.4 |
| RP (a) | 2.0 ± 0.7 | 1.8 | 3.3 | 1.1 |
| RP (b) | 17.9 ± 6.1 | 16.3 | 27.6 | 10.0 |
| RD (a) | 9.0 ± 8.0 | 6.7 | 24.7 | 2.8 |
| RD (a) minus sample 2 | 5.1 ± 1.9 | 5.2 | 7.1 | 2.8 |
| RD (b) only 2 samples | 50.9 | -- | 69.8 | 32.0 |
| RW (a) | 10.5 ± 4.0 | 9.4 | 15.9 | 6.3 |


a. Non-wiped and wiped subgroups after one test cycle

Figure 45. Effect of repeated test cycles on visual appearance of phase 3 RM coating.

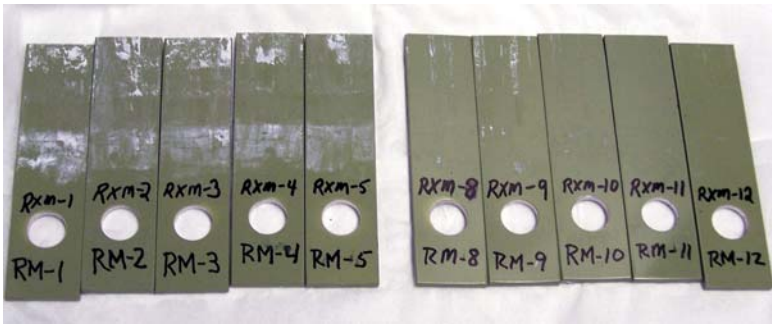


b. After two test cycles

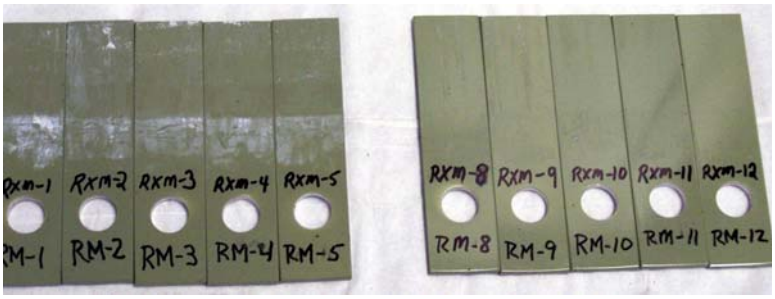


c. After three test cycles.

Figure 45 (cont'd). Effect of repeated test cycles on visual appearance of phase 3 RM coating.

## Analysis of Load-Time Response

The Kruskal-Wallis test indicates a significant statistical difference between the peak load performances among each of the RM, RP, and RD non-wiped "a" and wiped "b" groups in phase3. Peak loads for each of the non-wiped subgroups were not significantly different from the phase 1 RXM results, and the non-wiped RW peak loads were not significantly increased. Average work is compared for all coated sample groups and cycles in Figure 46, by strain rate. Corresponding average work for the phase 3 controls was 14.4 lb-in. at the low strain rate and 113 lb-in. at high strain. There were notable improvements in average work at both strain rates for all groups between cycles 1 and 3. The non-wiped RP(a) group yielded superior work performance at both strain rates in cycle 3 relative to all other groups and cycles. The removal of excess coating in early test cycles could explain optimal work in later cycles for the non-wiped groups, and photo documentation (Fig. 45) indicates the same potential mechanism could be acting for the wiped groups.

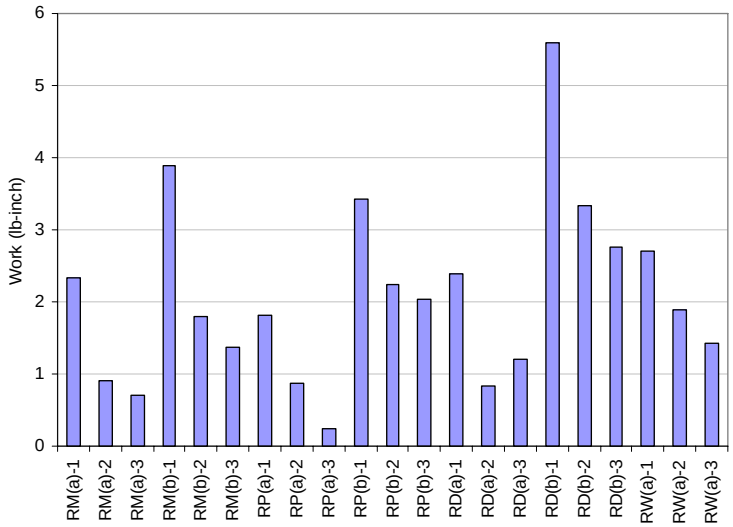


a. Low strain rate.

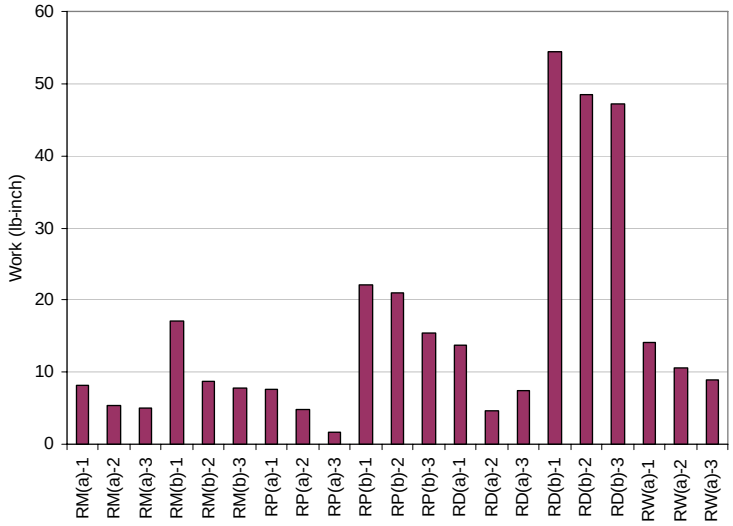


b. High strain rate.

Figure 46. Average work expended for each phase 3 sub-grouping and cycle.

Figure 47 gives average power measures for the coated sample groups in phase 3, showing identical trends and relative values to those of average work. The average power needed for the phase 3 controls, 1.6 lb-in./min. at low strain and 25.7 lb-in./min. at high strain, provides a basis for comparison. The average short-term variability of the load or "stick–slip" of the RM groups in phase 3 are presented in Figure 48 for both strain rates

and all cycles. Like phase 1 and phase 2 Rain-X samples, the phase 3 RM coating displayed consistently larger average standard deviations at low versus high strain rate, no strong trends over the three cycles, and comparable or slightly smaller values.

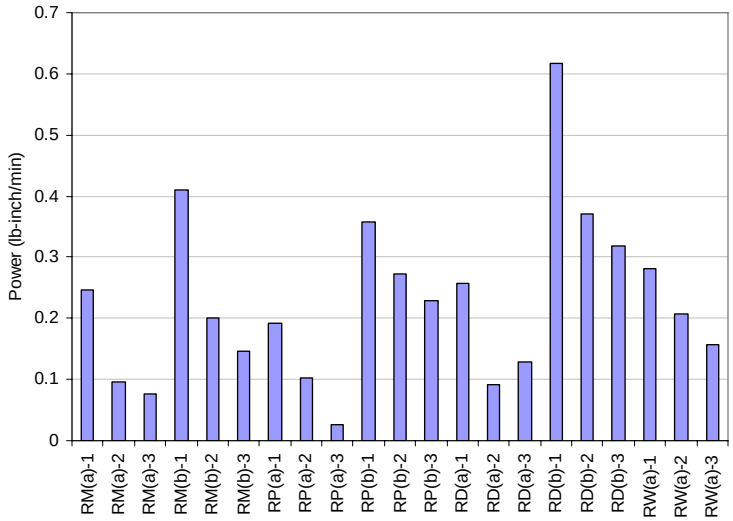


a. Low strain rate

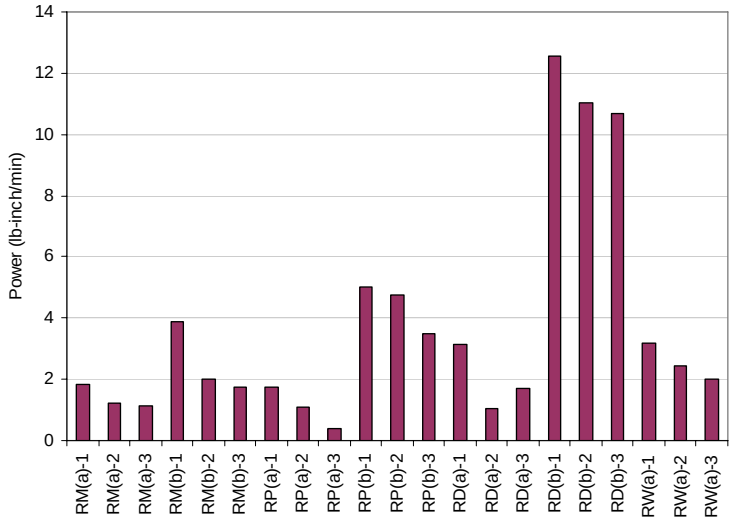


b. high strain rate.

Figure 47. Average power expended for each phase 3 subgrouping and cycle.

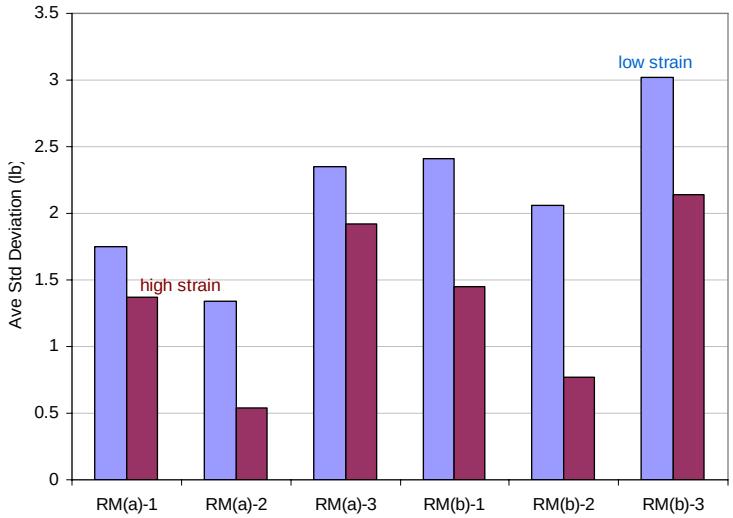


Figure 48. Average standard deviation (lb) from the mean load over successive 12-second intervals by strain rate in phase 3 RM tests, and averaged again for each RM subgroup and cycle.

## Phase 3 Conclusions

The adhesion performance of the RM(a) and RP(a) groups generally improved from cycle 1 to cycle 3. With RM-02 discounted, the cycle-3 adhesion performance of these samples taken as a single group was superior to even the cycle-3 performance of the best RXM samples from phase 1 (Table 6). The wiped RM(b) and RP(b) groups also improved in performance with cycling, though the incremental decreases in work are smaller than for the non-wiped samples. The non-wiped RD(a) and RW(a) subgroups also improved between cycles 1 and 2, and then held steady in cycle 3. Rewetting the coating mixture with IPA after drying caused a slight loss in performance, and washing the coating in a water stream after curing caused a slightly larger loss. Results of these tests indicate that the loss in performance caused by wiping off the coating is very sensitive to cure time prior to wiping. More tests of cure time effects are needed to better understand and minimize this loss.

## XPS, Contact Angle, and SEM–EDS Analyses

X-ray photoelectron spectroscopy (XPS) also called electron spectroscopy for chemical analysis (ESCA) is a chemical surface analysis method. XPS measures the chemical composition of the outermost 100 Å of a sample. Measurements can be made at greater depths by ion sputter etching to remove surface layers. All elements except for H and He can be detected at

concentrations above 0.05 to 1.0 atom %, depending on the element. In addition, chemical bonding information can be determined from detailed analysis.

Trigwell and Calle (2006) reported on XPS measurement of fluorocarbon, the principal component of the Rain-X–MP55 coating, remaining on the surface of coupons RM-01, RM-02, and RM-03 following three cycles of phase 3 testing. These measurements were compared with similar measurements of RM-07, a coupon from the same group that had never been tested, and Koropon control coupons, both uncoated and coated with plain Rain-X. Within experimental parameters, the surface compositions of RM-01 to -03 were similar and totally different from the controls. Also, the cycled coupon surfaces contained less MP55 than that of the untested coupon, indicating a loss of some of the coating. However, a significant amount of coating remained on the surfaces, and the ice adhesion performance had not been compromised. Consistent with the observed loss of coating at each test cycle, these results suggest that the failure plane between the coupons and the ice occurred within the coating.

Ten droplets of deionized water were placed along the length of each of these same coupons for contact angle analysis (Trigwell and Calle 2006). Mean angle ± standard deviation obtained for the Koropon control was 81° ± 3.3°, increasing to 104° ± 1.8° for the control with the Rain-X coating. In contrast, the tested samples were 137° ± 6.6°, 142° ± 8.2°, and 137° ± 11.9°, respectively, and untested RM-07 was 143° ± 10.9°. Contact angle data concur with the XPS result that MP-55 remains present on the tested coupon surfaces, and indicate that the hydrophobic performance of the untested surface is largely preserved after three test cycles.

Scanning electron microscopy (SEM) coupled with an energy dispersive spectroscopy (EDS) elemental map of fluorine was used to visualize conditions on Rain-X–MP-55 coated coupon surfaces. A test coupon was thinly coated and left to cure for more than 2 days prior to analysis, abrasive wiping, and re-analysis. Figure 49a shows evenly dispersed MP-55 throughout the coating of the non-wiped coupon with particle agglomerations present. The repeat SEM-EDS map in t Figure 49b, obtained after abrasive wiping of the coupon, once again shows the MP-55 to be well dispersed on the surface without significant agglomerations present. The abrasive wipe did not remove Teflon from the surface of the sample. The diameters of the MP-55 beads, measured by the SEM, fall below the wavelength of visible

light. This result infers that, though it may appear that the coating has been removed, it actually remains present. These SEM results verifying the presence of MP-55 on the coupon surface following abrasion support those of the XPS and contact angle analyses of tested coupons.

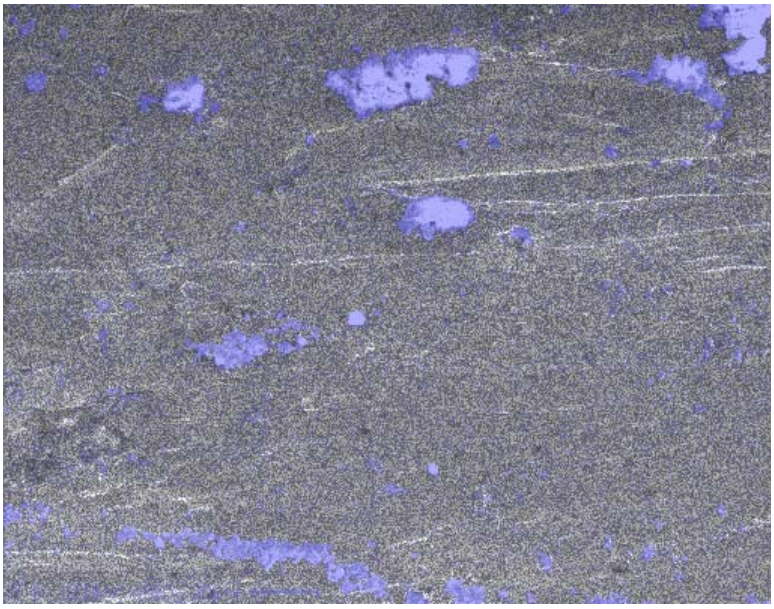

a. Thin coating of Rain-X–MP-55 after more than 2 days of curing,.

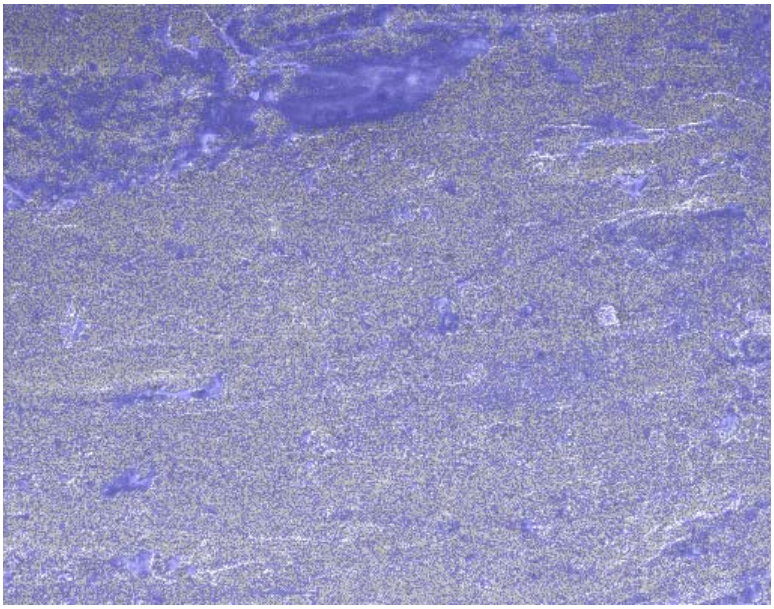

b. Re-analysis of the same coupon following abrasive wiping.

Figure 49. Fluorine overlay (blue tint) on SEM image of coupon surfaces.

# 9 Conclusions and Recommendations

Criteria for the experiment selected for this study were that it must discriminate between the effectiveness for reducing ice adhesion of several candidate coatings, each with distinct properties, and discern and quantify optimum performance. The double lap shear test following ASTM (2002) D3528-96 provided consistent load response patterns in preliminary tests of uncoated coupons and peak loads at failure that could exceed 1000 lbf. On the basis of these results, double lap shear testing was selected to evaluate and quantify coating performance. Measured $LO_2$ bracket temperatures obtained by NASA indicated that most of the temperature decrease in response to cryogenic fuel loading occurred over a 6-hour period at an average rate of 16–17°C/hr (29–31°F/hr). Bracket surface temperatures continued to decrease over 8+ hours, asymptotically approaching a minimum of –112°C (–170°F). The CRREL experiments used ice that was initially grown as strong and consistently as possible before being subjected to temperature decreases comparable to those of the prototype bracket. The test temperature condition was constant and equal to that of the bracket surface.

The double lap shear-testing program evolved in three primary phases. The first phase quantitatively evaluated the performance of a wide range of candidate coating materials. Phase 1 tests showed that Rain-X mixed with "maximum" MP-55 (RXM) was an outstanding coating to reduce ice adhesion to Koropon coated aluminum at cryogenic temperatures. Significant amounts of coating retained on the ice surface after each test indicated failure in the coating and the potential for loss of effectiveness with repeated cycles of ice formation and release. As RXM coating durability was not established in phase 1, further evaluation was needed to assess and minimize this uncertainty.

The purpose of the phase 2 investigations was to evaluate potential modifications to the RXM coating that would enhance durability and maintain effectiveness. The addition of DF 1040 in phase 2 to the original Rain-X–MP-55 maximum mixture did not improve the ice adhesion performance at cryogenic temperature or coating durability. Like the original, coating material was lost in each test cycle with all DF 1040 mixes. However, effectiveness of the remaining coating improved through three cycles and then

remained constant in cycle 4. Comparison of the 0% DF 1040 phase 2 and RXM–RXT phase 1 results indicate that the DC 1200 primer slightly degraded the performance of the original coating.

The third phase evaluated handling, application, resistance to weathering by a water stream, and durability of the RXM coating. Again, a progressive loss of coating material from the phase 3 coupons was evident through the test cycles, even for the wiped coupons. This loss of coating material was again accompanied by improved adhesive performance of the remaining coating. The adhesion performance of the RM(a) and RP(a) groups generally improved from cycle 1 to cycle 3. The cycle 3 performance of these subgroups was superior to even the cycle 3 performance of the best RXM samples from phase 1. The wiped RM(b) and RP(b) groups also improved in performance with cycling, though incremental decreases in work were smaller than for the non-wiped samples. The non-wiped RD(a) and RW(a) groups also improved between cycles 1 and 2, and then remained constant in cycle 3. Re-wetting the coating mixture with IPA after drying caused a slight loss in performance, and washing the coating in a water stream after curing caused a slightly larger loss. The phase 3 tests indicated that the loss of performance caused by wiping off the coating is very sensitive to cure time prior to wiping.

XPS measurement of fluorocarbon, a principle component of the Rain-X–MP55 coating, remaining on the surface of coupons RM-01, RM-02, and RM-03 following three test cycles were compared with similar measurements of RM-07, a coupon from the same group that had never been tested. Surface chemistry of Koropon control coupons, both uncoated and coated with plain Rain-X, was also mapped with XPS. The surface compositions of RM-01 to -03 were similar within experimental parameters, but totally different than the controls. The cycled coupons retained less MP55 than the untested coupon, indicating a loss of coating, but a significant amount of coating remained on the surfaces. Consistent with the observed loss of coating at each test cycle, these results suggest that the failure planes between the coupons and the ice occur within the coating. Contact angle analysis along the length of each of these same coupons provided data that concurred with the XPS results. The hydrophobic performance of the untested surface was largely preserved after three test cycles, indicating that MP-55 remained present on the tested coupon surfaces. Finally, SEM-EDS mapping of an abraded coupon surface also showed the presence of well-dispersed MP-55 maintaining a continuous coating.

The results of this investigation suggest the need for several follow-up studies to refine the optimal coating formulation, mixing, and application procedures. The overall consistency and performance of the BUM coating in phase 1 indicated superiority of UF-8TA over MP-55 when mixed with Braycote. As UF-8TA was not mixed with Rain-X, this change in Teflon powder added offers potential performance and consistency improvements to the coating. Also, reaction processes and environmental durability must be better understood. Wiping off excess coating after adequate curing offers the potential to achieve optimal performance without cycling. More investigation of cure time effects is needed if this benefit is to be achieved. Additional test cycles beyond those done in this program must eventually compromise the integrity and performance of the coating, and this "effectiveness limit" should be known. A parallel approach, using both double lap shear testing and XPS surface analysis to quantify surface chemistry and coating profile thickness changes with cycling, is a proven approach that offers the capability to resolve these remaining issues.

# 10 References

ASTM (2003) D3164-03, Standard test method for strength properties of adhesively bonded plastic lap-shear sandwich joints in shear by tension loading. In *Annual Book of ASTM Standards*. West Conshohocken, Pennsylvania: American Society for Testing and Materials.

ASTM (2002) D3528-96, Standard test method for strength properties of double lap-shear adhesive joints by tension loading. In *Annual Book of ASTM Standards*. West Conshohocken, Pennsylvania: American Society for Testing and Materials.

Deweese, D., M. Prince, K. McDougal, S. Davis, S. Chandler, and E. Martinez (2006) Developmental tests of the relative performance of coatings on reducing ice adhesion strength. Huntsville, AL: NASA Marshall Space Flight Center.

Siegel, S. and N. J. Castellan, Jr. (1988) *Nonparametric Statistics for the Behavioral Sciences.* New York, NY: McGraw-Hill.

Trigwell, S. and C. I. Calle (2006) Surface analysis of ice phobic coatings. NASA Kennedy Space Center, ESPL-TR06-001.

Zar, J. H. (1999) *Biostatistical Analysis.* Upper Saddle River, NJ: Prentice-Hall.

# REPORT DOCUMENTATION PAGE

*Form Approved*
*OMB No. 0704-0188*



**1. REPORT DATE** *(DD-MM-YYYY)*
May 2006

**2. REPORT TYPE**

**3. DATES COVERED** *(From - To)*

**4. TITLE AND SUBTITLE**

Double Lap Shear Testing of Coating Modified Ice Adhesion to Liquid Oxygen Feed Line Bracket, Space Shuttle External Tank

**5a. CONTRACT NUMBER**
NNL05AA401

**5b. GRANT NUMBER**

**5c. PROGRAM ELEMENT NUMBER**

**6. AUTHOR(S)**

M.G. Ferrick, N.D. Mulherin, R.B. Haehnel, B.A. Coutermarsh, G.D. Durell, T.J. Tantillo, T.L. St. Clair, E.S. Weiser, R.J. Cano, T.M. Smith, and E.C. Martinez

**5d. PROJECT NUMBER**

**5e. TASK NUMBER**

**5f. WORK UNIT NUMBER**

**7. PERFORMING ORGANIZATION NAME(S) AND ADDRESS(ES)**

Cold Regions Research and Engineering Laboratory, U.S. Army Engineer Research and Development Center, 72 Lyme Rd, Hanover, NH; National Institute of Aerospace, Hampton, VA; NASA Langley Research Center, Hampton, VA; NASA John F. Kennedy Space Center, KSC, FL; Lockheed Martin Space Systems, MSFC, AL

**8. PERFORMING ORGANIZATION REPORT NUMBER**

ERDC/CRREL TR-06-11

**9. SPONSORING / MONITORING AGENCY NAME(S) AND ADDRESS(ES)**

National Aeronautics and Space Administration
Washington, DC

**10. SPONSOR/MONITOR'S ACRONYM(S)**

**11. SPONSOR/MONITOR'S REPORT NUMBER(S)**

**12. DISTRIBUTION / AVAILABILITY STATEMENT**

Approved for public release; distribution is unlimited.

**13. SUPPLEMENTARY NOTES**

**14. ABSTRACT**

The brackets that secure the liquid oxygen feed line to the external tank are known locations of frost and ice growth during the period following fuel loading. This experiment quantified the reduced adhesion when ice phobic coatings were applied to test coupons simulating the bracket surface. Double lap shear testing of coated and uncoated coupons provided robust test specimens and consistent load response patterns with exceptional resolution. For these tests ice was grown as strong and consistently as possible, subjected to temperature decreases comparable to those of the prototype bracket, and tested at a controlled temperature of –112ºC. The tests evolved in three phases, with uncoated controls included in each group of tested samples. The first phase of testing evaluated a wide range of coatings, and showed that Rain-X mixed with MP-55 powdered Teflon (RXM) was an outstanding coating to reduce ice adhesion to Koropon coated aluminum. However, significant amounts of coating were retained on the ice surface following each test, indicating failure in the coating and potential loss of effectiveness with repeated ice formation and release. Phase 2 evaluated potential modifications to RXM that might maintain effectiveness and enhance durability. However, the modified RXM mixtures did not improve the ice adhesion performance or coating durability. Phase 3 evaluated the effects of handling, application, resistance to weathering by water, and durability of the RXM coating. Coating material was again progressively lost through the repeat test cycles, but performance generally improved. Results also indicated that cure times longer than 1.5 hr prior to coating disturbance are needed for optimal performance. The MP55 remaining on the surface of three coupons after three cycles of testing, and on one untested coupon from the same group, was measured with XPS. The tested coupons retained slightly less MP55 than the untested coupon, indicating a minor loss of coating. Contact angle analysis of these same coupons showed that the hydrophobic performance of the tested surfaces was largely preserved. Scanning electron microscopy with an energy dispersive spectroscopy elemental map indicated that the MP-55 was evenly dispersed throughout the coated surface, and abrasive wiping did not remove a significant portion of the Teflon. Follow-up studies to refine the optimal coating formulation, mixing, and application procedures, including cure time, are necessary. Phase 1 testing indicated superiority of UF-8TA powdered Teflon over MP-55 when mixed with Braycote.

**15. SUBJECT TERMS**

Double lap shear testing
cryogenic temperatures
ice adhesion
ice phobic coatings
Space Shuttle

| **16. SECURITY CLASSIFICATION OF:** | | | **17. LIMITATION OF ABSTRACT** | **18. NUMBER OF PAGES** | **19a. NAME OF RESPONSIBLE PERSON** |
|---|---|---|---|---|---|
| **a. REPORT** | **b. ABSTRACT** | **c. THIS PAGE** | | | **19b. TELEPHONE NUMBER** *(include area code)* |
| U | U | U | U | 91 | |

**Standard Form 298 (Rev. 8-98)**
**Prescribed by ANSI Std. 239.18**

**14. ABSTRACT (cont'd).**

As UF-8TA was not mixed with Rain-X, this change in Teflon powder might offer performance and consistency improvements to the coating. Also, reaction processes and environmental durability of the final coating must be better understood. Double lap shear testing and XPS analysis can quantify ice adhesion and coating profile thickness changes with cycling, and is a proven approach to resolve these remaining issues.